Research Square

Preprints are preliminary reports that have not undergone peer review.
They should not be considered conclusive, used to inform clinical practice,
or referenced by the media as validated information.

# HIF-2α Drives NF-κB–NLRP3–Dependent Inflammatory Lung Injury Following Trauma

**Madathilparambil V Suresh**

madathil@umich.edu

**Sumeet Solanki**
**Cristina Castillo**
**Nemanja Bratic**
**Nahush Keshav**
**Andrew Benjamin**
**David Burmeister**
**Bethany Moore**
**Yatrik M. Shah**
**Krishnan Raghavendran**

**Research Article**

**Keywords:** HIF-2α, Lung contusion, Type II AEC, NF-κB, Porcine

**Posted Date:** November 16th, 2026

**DOI:** https://doi.org/10.21203/rs.3.rs-11586096/v1

**License:** This work is licensed under a Creative Commons Attribution 4.0 International License.
Read Full License

**Additional Declarations:** No competing interests reported.

# HIF-2α Drives NF-κB–NLRP3–Dependent Inflammatory Lung Injury Following Trauma

Madathilparambil V. Suresh[1], Sumeet Solanki[3], Cristina Castillo[3], Nemanja Bratic[1], Nahush Keshav[1], Andrew Benjamin[1], David M. Burmeister [4], Bethany Moore[2], Yatrik M. Shah[3], Krishnan Raghavendran[1]

[1]Department of Surgery, University of Michigan, Ann Arbor, MI, USA

[2]Department of Molecular & Integrative Physiology, University of Michigan, Ann Arbor, MI, USA

[3]Department of Microbiology and Immunology, University of Michigan, Ann Arbor, MI, USA.

[4]Department of Medicine, F. Edward Hébert School of Medicine, Uniformed Services University of the Health Sciences, Bethesda, Maryland, USA

**Running Title:** HIF-2α Drives Inflammation After Lung Contusion

**Keywords**: HIF-2α, Lung contusion, Type II AEC, NF-κB, Porcine

*Corresponding authors

1. Madathilparambil V. Suresh
   Associate Research Scientist
   University of Michigan
   Ann Arbor, MI 48109, USA
   Phone: +1-734-747-2055
   Email: madathil@med.umich.edu

2. Dr. Krishnan Raghavendran, MD
   Professor of Surgery
   Department of Surgery,
   University of Michigan
   Ann Arbor, MI 48109, USA
   Phone: +1-734-647-9693
   Email: kraghave@med.umich.edu

**Abstract**

Lung contusion (LC) is a common consequence of blunt thoracic trauma and a major risk factor for acute respiratory distress syndrome (ARDS). Although tissue hypoxia is a hallmark of LC, the mechanisms linking hypoxic signaling to persistent inflammation and lung injury remain incompletely understood. We investigated the role of hypoxia-inducible factor-2α (HIF-2α), encoded by *EPAS1*, using a translational approach combining human and porcine-contused lung tissues, a murine model of isolated LC with alveolar epithelial cell-specific HIF-2α deletion, a bacterial pneumonia model, and in vitro macrophage studies. Postmortem human contused lung tissues showed increased HIF-2α expression in the alveolar epithelium, consistent with published single-cell transcriptomic data demonstrating increased *EPAS1* expression in epithelial cells and macrophages from injured lungs. In a porcine model of combined hemorrhagic shock and pulmonary contusion, HIF-2α expression was increased in contused regions compared with uninjured regions of the same animal. In mice, conditional deletion of HIF-2α in type II alveolar epithelial cells reduced bronchoalveolar lavage albumin levels, attenuated injury-associated changes in lung mechanics, and decreased inflammatory cytokine and chemokine production. These effects were accompanied by reduced NF-κB, NLRP3 inflammasome-associated, and VEGFA signaling. Mice lacking epithelial HIF-2α also exhibited improved survival following lethal *Klebsiella pneumoniae* challenge. In macrophages, pharmacological HIF stabilization enhanced inflammatory gene expression, whereas selective HIF-2α inhibition with PT2385 reduced IL-1β promoter activity and caspase-1 activation. Collectively, these findings implicate HIF-2α in the regulation of inflammatory signaling and lung injury following trauma and support further investigation of HIF-2α-dependent pathways as potential therapeutic targets in ARDS.

| Abbreviation | Full term |
|---|---|
| AECII | Alveolar epithelial type II cell |
| ALI | Acute lung injury |
| ARDS | Acute respiratory distress syndrome |
| BAL | Bronchoalveolar lavage |
| BALF | Bronchoalveolar lavage fluid |
| BMDM | Bone marrow-derived macrophage |
| CFU | Colony-forming unit |
| EPAS1 | Endothelial PAS domain protein 1 |
| FG-4592 | Roxadustat, a HIF stabilizer |
| GLUT1 | Glucose transporter 1 |
| HIF | Hypoxia-inducible factor |
| HIF-1α | Hypoxia-inducible factor-1 alpha |
| HIF-2α | Hypoxia-inducible factor-2 alpha |
| HRE | Hypoxia-response element |
| IF | Immunofluorescence |
| IL-1β | Interleukin-1 beta |
| IL-6 | Interleukin-6 |
| KC | Keratinocyte chemoattractant (CXCL1) |
| KP | *Klebsiella pneumoniae* |
| LC | Lung contusion |
| MCP-1 | Monocyte chemoattractant protein-1 |
| MIP-2 | Macrophage inflammatory protein-2 (CXCL2) |
| NF-κB | Nuclear factor kappa B |
| NLRP3 | NOD-, LRR-, and pyrin domain-containing protein 3 |
| PC | Pulmonary contusion |
| PT2385 | Selective HIF-2α antagonist |
| qPCR | Quantitative polymerase chain reaction |
| RAGE | Receptor for advanced glycation end products |
| RNA | Ribonucleic acid |
| RT-qPCR | Reverse transcription quantitative polymerase chain reaction |
| SP-C | Surfactant protein C |
| TGF-β | Transforming growth factor beta |
| TNF-α | Tumor necrosis factor alpha |
| VEGFA | Vascular endothelial growth factor A |
| WES | Wes automated capillary Western blot system |
| WT | Wild type |

## Introduction

Lung contusion (LC) is a frequent consequence of blunt thoracic trauma and remains a major contributor to acute respiratory distress syndrome (ARDS) after both civilian and military injuries (1, 2). LC disrupts the alveolar-capillary barrier, resulting in pulmonary edema, hypoxemia, reduced lung compliance, and inflammatory cell infiltration (3-5). In addition to direct tissue damage, patients with LC are at increased risk of secondary complications, including ventilator-associated pneumonia and progressive acute lung injury (ALI) (6-10). Although supportive care has improved outcomes, the mechanisms linking tissue hypoxia to persistent inflammation and lung injury following LC remain incompletely understood.

Because LC disrupts alveolar oxygen exchange, significant tissue hypoxia develops early after injury, which activates hypoxia-inducible factors (HIFs), a family of transcription factors that regulate cellular adaptation to reduced oxygen availability (11, 12). HIFs consist of oxygen-regulated α subunits and a constitutively expressed β subunit (13). Under normoxic conditions, HIF-α proteins are rapidly degraded, whereas hypoxia stabilizes these proteins, allowing them to translocate to the nucleus and regulate genes involved in inflammation, metabolism, angiogenesis, and cell survival (14, 15). While HIF-1α has been extensively studied in acute inflammatory lung injury, emerging evidence suggests that HIF-2α regulates distinct transcriptional programs in epithelial and myeloid cells. Its contribution to post-traumatic lung inflammation, however, remains poorly understood. *EPAS1* is expressed at high levels in the lung relative to other organs (16), and HIF-2α is essential for surfactant production by alveolar type II epithelial cells during lung maturation (17). HIF-2α protein has also been detected in distinct pulmonary cell populations under hypoxic conditions (18). Previous studies suggest that HIF-2α has context-dependent effects in pulmonary disease, contributing to inflammatory signaling, pulmonary hypertension, epithelial repair, and macrophage activation (19-22). Notably, sustained HIF signaling in airway-derived epithelial progenitors has been implicated in impaired alveolar repair and pathological remodeling in idiopathic pulmonary fibrosis, and selective HIF-2α inhibition has been proposed as a potential strategy to restore functional repair (23).

To further characterize EPAS1 expression across pulmonary cell populations, we analyzed single-cell RNA-sequencing data provided by McCall et al.(23). Alveolar epithelial cells and macrophages are important contributors to the inflammatory response following LC. Activation of these cells promotes the release of cytokines and chemokines, including IL-1β, IL-6, TNF-α, KC,

and MIP-2, which contribute to neutrophil recruitment, increased vascular permeability, and progression to ARDS (24-26). Among the pathways involved, NF-κB and the NLRP3 inflammasome are important mediators of inflammatory lung injury and IL-1β production (25). Previous studies have also linked HIF-2α to the regulation of NF-κB and NLRP3-associated inflammatory responses (16, 21). However, whether HIF-2α contributes to these inflammatory pathways following LC remains unclear.

Despite the recognized importance of hypoxia in lung contusion, the contribution of HIF-2α to post-traumatic inflammatory lung injury remains incompletely understood. We hypothesized that HIF-2α contributes to inflammatory lung injury following LC and is associated with NF-κB- and NLRP3-related inflammatory signaling. To investigate this, we combined analyses of human lung contusion specimens, published single-cell transcriptomic data, a porcine model of hemorrhagic shock with pulmonary contusion, a murine model of LC using conditional deletion of HIF-2α in alveolar epithelial cells, and complementary mechanistic studies in macrophages.

Our findings provide evidence that HIF-2α contributes to pulmonary permeability changes, inflammatory cytokine production, and inflammatory signaling following traumatic lung injury and support further investigation of HIF-2α-dependent pathways as potential therapeutic targets in ALI and ARDS.

## Materials and Methods

### Human Lung Specimens

Deidentified postmortem human lung specimens were obtained from the Heart and Lung Institute at the University of British Columbia under protocols approved by the University of British Columbia Research Ethics Board. Their use followed institutional guidelines and the principles of the Declaration of Helsinki.

### Animals

All murine procedures were approved by the Institutional Animal Care and Use Committee (IACUC) at the University of Michigan (Protocol No. PRO00011624, “Inflammatory Biology of Direct Lung Injury”). All swine procedures were approved by the IACUC of the Uniformed Services University of the Health Sciences and were performed at an AAALAC-accredited facility. All procedures complied with the Animal Welfare Act, the *Guide for the Care and Use of Laboratory Animals*, NIH guidelines, and applicable state and federal regulations.

Age-matched male and female SP-C-rtTA/tetO-CMV-Cre/HIF-2α^fl/fl mice (6–8 weeks old) were used. Conditional HIF-2α deletion in alveolar type II epithelial cells was induced by doxycycline administration. Mice not receiving doxycycline served as controls. Equal numbers of males and females were included in each experimental group. Because the study was not designed or powered to detect sex-by-treatment interactions, sex-stratified analyses were not performed. In total, 108 mice and 4 pigs were used in this study. Where possible, tissues collected from the same mouse were used for multiple assays; therefore, the sum of sample sizes reported across figures exceeds the total number of animals used.

**Animals and generation of conditional HIF-2α knockout mice**

Age-matched male and female mice aged 7–8 weeks were used. Triple-transgenic mice carrying the SP-C-rtTA^+/tg^, $(tetO)_7$-CMV-Cre^+/tg^, and HIF-2α^flox/flox^ alleles were generated as previously described (24). These mice permit doxycycline-inducible, type II alveolar epithelial cell-specific deletion of HIF-2α. To induce recombination, mice were fed doxycycline-containing chow (625 mg/kg) and provided drinking water containing doxycycline (0.8 mg/mL), following the regimen established in previous studies of alveolar epithelial cell-specific HIF-1α deletion. Doxycycline treatment was discontinued 7–10 days before lung contusion. Doxycycline-treated mice are designated HIF-2α (−/−), whereas untreated littermate control mice, maintained on regular chow and drinking water without doxycycline, are designated HIF-2α (+/+). All mice were housed under identical conditions. All procedures were approved by the Institutional Animal Care and Use Committee (IACUC) of the University of Michigan.

**Genotyping.**

Genotyping of HIF-2α floxed, Cre, and SP-C-rtTA transgenic mice was performed and confirmed by Transnetyx (Cordova, TN) according to the manufacturer's protocols. The HIF-2α floxed allele was detected using the forward primer 5′-GAGAGCAGCTTCTCCTGGAA-3′ and reverse primer 5′-TGTAGGCAAGGAAACCAAGG-3′ (HIF2-2), yielding 220-bp and 182-bp products for the floxed and wild-type alleles, respectively. The Cre and SP-C-rtTA transgenes yielded products of 370 bp and 350 bp, respectively.

**Swine**.

Pigs were obtained from Animal Biotech Industries Inc. (Doylestown, PA) and acclimated for 24 h before experiments**.**

**Group allocation**

Experimental groups were defined by genotype, an inherent characteristic of the animal that cannot be randomly assigned. HIF-2α (+/+) and HIF-2α (−/−) mice were assigned to their respective groups based on genotyping performed before each experiment. Within each genotype, animals were assigned to injury conditions and post-injury time points according to animal availability. No formal randomization was performed.

In the porcine model, all animals underwent the same combined hemorrhage and pulmonary contusion protocol and served as their own regional controls, with comparisons made among contralateral, adjacent ipsilateral, and injured lung regions. Therefore, separate group allocation was not applicable. The absence of formal randomization in the murine experiments is acknowledged as a study limitation.

**Murine Model for Lung Contusion**

Lung contusion (LC) was induced in anesthetized mice using a cortical contusion impactor as previously described (27-31). Mice were positioned in the left lateral decubitus position, and a controlled impact was delivered to the right thorax along the posterior axillary line. Animals recovered spontaneously and were studied at designated time points after injury.

**Porcine Model of Lung Contusion**

Adult Yorkshire swine (n = 4; 2 male, 2 female; 55.0 ± 2.4 kg) were subjected to unilateral closed-chest pulmonary contusion in the setting of controlled hemorrhagic shock, as previously described (32-34). Briefly, animals were fasted for 12 hours prior to the study and induced with 4–8 mg/kg Telazol IM, after which they were transported to the operating room and maintained on 1–5% inhaled isoflurane. Animals were intubated with a 5.0–6.0 mm endotracheal tube and mechanically ventilated using tidal volumes of 7–10 mL/kg and a respiratory rate of 10–15 breaths per minute to maintain end-tidal carbon dioxide at 40 ± 5 mmHg. Saline was initiated at 2 mL/kg/hr through an established ear catheter, and warming blankets were used to maintain core temperature between 36.5 and 39.5°C.

Carotid and femoral arteries were accessed percutaneously using 5–7 Fr catheters following needle and guidewire placement in a modified Seldinger technique. One catheter was used for continuous blood pressure monitoring, while the other was used to induce controlled hemorrhage corresponding to 40% of the estimated blood volume. Hemorrhage was performed prior to pulmonary contusion to establish hemorrhagic shock and systemic hypoperfusion before the pulmonary insult, reproducing the clinically relevant setting in which blood loss and thoracic

injury occur together. Hemorrhage was completed at a constant rate of over 40 minutes using an automated Masterflex L/S Digital Miniflex Pump (Cole-Parmer, Vernon Hills, Illinois).

Toward the end of the hemorrhage period, pulmonary contusion (PC) was induced using a captive-bolt stun gun designed for concussion stunning (Schermer KC Stunner, Karl Schermer, Paderborn, Germany). The bolt gun was positioned against the distal third of the right hemithorax and fired using C-5 Red 22-gauge charges. One hour after pulmonary contusion, animals were humanely euthanized by phenobarbital infusion in accordance with AVMA guidelines. This model was designed to characterize the acute pulmonary response to combined hemorrhage and contusion; the 1-hour endpoint does not permit assessment of the subsequent progression or resolution of lung injury. Because all animals underwent both hemorrhage and contusion, shock-only and contusion-only control groups were not included, and the independent contributions of each insult cannot be distinguished in this model. Lung tissue samples were collected from the contused region, adjacent ipsilateral non-contused lung tissue, and the contralateral lung for histological and protein analyses.

**Lung Pressure-Volume Mechanics**

Immediately following blood collection, pulmonary respiratory mechanics were assessed. Mice were then further exsanguinated by transection of the abdominal inferior vena cava. An 18-gauge metal cannula was inserted into the trachea through a midline cervical incision, and the animals were connected to a FlexiVent system (SCIREQ, Montreal, QC, Canada) for ventilation and data acquisition. Postmortem ventilation was performed at a tidal volume of 10 mL/kg, a respiratory rate of 150 breaths/min, and a positive end-expiratory pressure of 2 $cmH_2O$. Pressure-volume maneuvers were performed using a volume-controlled pressure-volume ramp consisting of controlled inflation and deflation to assess quasi-static lung compliance, as previously described (35).

**Determination of Cytokine and Chemokine Levels in BAL Fluid.**

Bronchoalveolar lavage (BAL) fluid was collected for measurement of albumin, inflammatory cytokines and chemokines, and differential cell counts. Cytokine and chemokine levels in BAL fluid, including IL-1β, IL-6, TNF-α, KC, MIP-2, MCP-1, and MCP-5, were quantified by ELISA (36, 37).

**Cytospin cell count**

Bronchoalveolar lavage (BAL) cells were centrifuged at 600 × g for 5 minutes using a Cytospin II (Shandon Scientific, Pittsburgh, PA, USA). Cytospin preparations were stained with Diff-Quik (Dade Behring Inc., Newark, DE, USA) according to the manufacturer's instructions and examined under a light microscope at 20× magnification. Differential inflammatory cell counts were determined based on standard morphological criteria, including macrophages, neutrophils, and lymphocytes (35).

**Human Lung Histology and Immunostaining**

Human lung contusion specimens were obtained from the Heart and Lung Institute, University of British Columbia, Vancouver, Canada. Lungs were fixed in 10% neutral-buffered formalin, embedded in paraffin, and sectioned at 5 μm. Tissue sections were stained with hematoxylin and eosin (H&E) as previously described. Histological changes were evaluated by light microscopy, including alveolar structural disruption, inflammatory cell infiltration, and interstitial alterations.

For immunostaining, paraffin-embedded lung tissue sections were processed to evaluate HIF-2α expression and localization using a goat anti rabbit polyclonal HIF-2α antibody (NB100-122, Novus Biologicals; 1:2000 dilution), followed by an appropriate secondary antibody.

**Murine and Porcine Lung Histology and Image Analysis**

Lungs were fixed in 10% neutral-buffered formalin, embedded in paraffin, sectioned at 5 μm, and stained with hematoxylin and eosin (H&E) as previously described (31, 33). Lung injury in mice was scored using a modification of the ATS lung injury scoring system (Matute-Bello et al., 2011). Alveolar and interstitial neutrophils, hyaline membranes, proteinaceous debris, and alveolar septal thickening were assessed in five randomly selected fields per section at ×20 magnification. All mouse histological scoring was performed by an investigator blinded to genotype and injury condition.

Porcine lung injury was scored using a semiquantitative system developed for large-animal models of acute lung injury (38). Separate tissue samples from the contused, adjacent ipsilateral non-contused, and contralateral lung regions were evaluated. The investigator performing the porcine histological scoring was blinded to the lung region from which each tissue sample was collected.

**HIF-2α Immunofluorescence Staining**

Immunofluorescence staining was performed as previously described (35, 39). Briefly, 5-μm-thick paraffin-embedded human and mouse lung sections were deparaffinized and subjected to heat-induced epitope retrieval using 1× citrate buffer, pH 6.0 (Dako). Sections were blocked with 7%

bovine serum albumin, 1% fetal calf serum, and 0.05% sodium azide for 15 min, followed by overnight incubation at 4°C with an anti-HIF-2α primary antibody. Sections were then incubated with goat anti-rabbit Alexa Fluor 594-conjugated secondary antibody for 60 min at room temperature, with intermittent washes, and mounted with ProLong Gold Antifade Reagent containing DAPI (Invitrogen)

**Gene Expression**

Total RNA was isolated from whole-lung tissue and isolated type II alveolar epithelial cells. Gene expression was quantified by real-time quantitative PCR using TaqMan assays for IL-1β, IL-6, TNF-α, VEGFA, NF-κB, and NLRP3. Expression levels were normalized to GAPDH and calculated using the 2^-ΔΔCt method.

**Protein Expression – WES Analysis**

Protein expression was analyzed using the WES automated capillary Western blot system (Protein Simple, San Jose, CA, USA) according to the manufacturer's instructions, with a 12–230 kDa separation module (SM-W004) and an anti-rabbit detection module (DM-001). Lung lysates were diluted in 0.1× Sample Buffer (prepared by diluting 10× Sample Buffer 2 1:100), combined with 5× Fluorescent Master Mix, and denatured at 95°C for 5 min. Each capillary was loaded with 1 µg of total protein. Samples, blocking reagent, primary antibodies diluted in antibody diluent, HRP-conjugated secondary antibody, and chemiluminescent substrate were dispensed into the assay plate. HIF-2α was detected with a rabbit polyclonal anti-HIF-2α antibody (NB100-122, Novus Biologicals; 1:50), and GAPDH was detected as the loading control with a rabbit monoclonal anti-GAPDH antibody (14C10) 2118, Cell Signaling Technology; 1:50). Separation, immunodetection, and chemiluminescent signal acquisition were performed automatically by the instrument. Data was analyzed with Compass for Simple Western software [version]. HIF-2α peak area was normalized to GAPDH peak area, and apparent molecular weights were determined from the system's internal standards (35, 37).

**Isolation of Type II Alveolar Epithelial Cells**

Type II alveolar epithelial cells were isolated from injured and uninjured mouse lungs using Dispase digestion, sequential filtration, and negative selection with biotinylated anti-CD32 and anti-CD45 antibodies, as previously described (39). Cell preparations were >90% pure as determined by SP-C staining.

**Human Cell Culture**

Human lung epithelial cells and HEK293 cells were maintained under standard culture conditions and used for the indicated in vitro studies. HEK293 cells were obtained from ATCC.

**Macrophage Studies**

Bone marrow–derived macrophages (BMDMs) and RAW264.7 macrophages were exposed to hypoxia (1% $O_2$, 16 h) or treated with the HIF stabilizer FG-4592 (10 μM) in the presence or absence of the HIF-2α inhibitor PT2385 (10 μM). Following treatment, expression of inflammatory cytokines and hypoxia-responsive genes was assessed by quantitative real-time PCR. To evaluate HIF-dependent transcriptional activity, cells were transfected with IL-1β promoter luciferase reporter constructs and analyzed using dual-luciferase reporter assays as previously described (40).

**Inflammasome Activation**

Inflammasome activation was assessed in RAW264.7 macrophages by measuring caspase-1 cleavage using Western blot analysis following FG-4592 treatment or hypoxic exposure in the presence or absence of PT2385. Expression of the cleaved caspase-1 p20 subunit was used as a marker of inflammasome activation. Co-immunoprecipitation studies were performed to examine interactions between HIF-2α and NLRP3 as previously described (41, 42).

**Klebsiella pneumoniae Infection Model**

*Klebsiella pneumoniae* (KP) strain 43816 (serotype 2) was obtained from the American Type Culture Collection (Manassas, VA, USA) and cultured overnight in tryptic soy broth (Becton Dickinson, Franklin Lakes, NJ, USA). Serial dilutions were prepared to obtain a final inoculum of 500 colony-forming units (CFU) in 30 μL. Mice were inoculated with the bacterial suspension or vehicle control by deep oropharyngeal aspiration under isoflurane anesthesia, as previously described (37). This experiment was conducted as an independent model of infectious lung injury, without prior lung contusion, to investigate the role of epithelial HIF-2α in the response to *K. pneumoniae* infection. Survival was monitored for 10 days following inoculation. Animals were assessed every 8 hours, and predefined humane endpoint criteria were used to determine when euthanasia was required.

**Statistical Analysis**

Data are presented as mean ± SEM for continuous variables unless otherwise indicated. Ordinal histopathological injury scores are presented as median (IQR and range) and were analyzed using the Kruskal–Wallis test followed by Dunn's multiple-comparisons test (38). Comparisons between

two independent groups for continuous variables were performed using a two-tailed, unpaired Student's *t*-test with Welch's correction. For continuous outcomes involving more than two groups with a single factor, one-way analysis of variance (ANOVA) followed by Tukey's multiple-comparisons test was used. For continuous outcomes assessed across genotype and time, two-way ANOVA followed by Tukey's multiple-comparisons test was used. Kaplan–Meier survival curves were compared using the log-rank (Mantel–Cox) test. Statistical analyses were performed using GraphPad Prism version 11 (GraphPad Software, San Diego, CA, USA). All statistical tests were two-sided, and $P < 0.05$ was considered statistically significant.

**Results**

**Figure 1. HIF-2α is induced in human and experimental lung contusion**

Because lung contusion (LC) is associated with substantial tissue hypoxia (35), we first examined whether HIF-2α expression is altered following injury. Immunohistochemical analysis of postmortem human lung specimens revealed increased HIF-2α expression in contused lungs compared with uninjured lungs, with prominent localization to the alveolar epithelium (Figure 1A–B) (n = 3 per group). Consistent with these findings, immunofluorescence staining demonstrated minimal HIF-2α expression in uninjured lungs, whereas injured lungs exhibited increased HIF-2α signal within alveolar structures (Figure 1C–D) (n = 3 per group). To further characterize cell-specific EPAS1 expression, we analyzed single-cell RNA-sequencing data provided by McCall et al. (23) EPAS1 expression was increased in epithelial cells and macrophage populations associated with injured lungs (Figure 1E). We next examined HIF-2α expression in a murine model of LC. Lung contusion induced robust HIF-2α expression in control mice, whereas expression remained markedly reduced in mice with type II alveolar epithelial cell-specific HIF-2α deletion (Figure 1F–G) (n = 3 per group). Collectively, these findings demonstrate increased HIF-2α expression following human and experimental lung contusion and identify epithelial cells and macrophages as cell populations exhibiting increased EPAS1 expression.

**Figure 2. Generation and validation of epithelial HIF-2α–deficient mice**

To investigate the role of epithelial HIF-2α in lung injury, we generated mice with doxycycline-inducible deletion of HIF-2α in type II alveolar epithelial cells (HIF-2α^fl/fl^; SP-C-rtTA^+/tg^; $(tetO)_7$-CMV-Cre^+/tg^). Doxycycline administration induces Cre-mediated recombination, resulting in HIF-2α deletion in the respiratory epithelium. PCR genotyping confirmed the presence of the floxed HIF-2α allele and the SP-C-rtTA and Cre transgenes in the experimental mice (Figure

2A, B). Mice carrying the floxed allele and both transgenes following doxycycline treatment are referred to hereafter as HIF-2α (−/−) mice, whereas littermates lacking Cre served as HIF-2α (+/+) controls (n = 3 per group). Following doxycycline treatment, *Epas1* mRNA expression was reduced by approximately 50% in HIF-2α (−/−) lungs compared with controls (Figure 2C), accompanied by a reduction in HIF-2α protein detected by capillary Western blot (Figure 2D). Immunofluorescence analysis of uninjured lungs showed HIF-2α signal in the alveolar epithelium of HIF-2α (+/+) mice, with weaker staining in HIF-2α (−/−) mice (Figure 2E). Together, these findings support reduced HIF-2α expression following doxycycline-induced deletion in this model.

**Figure 3. Epithelial HIF-2α promotes lung injury following contusion**

To examine the role of epithelial HIF-2α in lung injury following contusion, HIF-2α (+/+) and HIF-2α (−/−) mice were subjected to LC and evaluated at different time points. Pressure–volume measurements showed altered pulmonary mechanics in HIF-2α (+/+) mice at 24 and 48 hours after injury, whereas these changes were less pronounced in HIF-2α (−/−) mice (Figure 3A; n = 6 per group). Histological analysis also showed more severe lung injury in HIF-2α (+/+) mice, with increased alveolar hemorrhage, inflammatory cell infiltration, and disruption of alveolar architecture at both points (Figure 3B; n = 3 per group). These changes were less pronounced in HIF-2α (−/−) mice. Bronchoalveolar lavage fluid analysis showed no significant difference in macrophage numbers between the groups. However, neutrophil numbers were higher in HIF-2α (+/+) mice than in HIF-2α (−/−) mice following LC (Figure 3C; n = 3 per group). Together, these findings suggest that epithelial HIF-2α contributes to pulmonary dysfunction, neutrophil recruitment, and lung injury following contusion.

**Figure 4. Epithelial HIF-2α promotes permeability injury and inflammation following contusion**

We examine the role of epithelial HIF-2α in alveolar-capillary barrier injury, BAL albumin levels were measured at different time points following LC. HIF-2α (−/−) mice had significantly lower BAL albumin levels than HIF-2α (+/+) mice at 5, 24, and 48 hours after injury, suggesting less disruption of the alveolar-capillary barrier (n = 10 per group) (Figure 4A). This difference was no longer apparent at 72 hours.

We next measured inflammatory mediators in BAL fluid. IL-6 and TNF-α levels increased following LC in HIF-2α (+/+) mice but were lower in HIF-2α (−/−) mice, particularly during the

early phase of injury (Figure 4B–C). The neutrophil-associated chemokines keratinocyte chemoattractant (KC/CXCL1) and macrophage inflammatory protein-2 (MIP-2/CXCL2) were also lower in HIF-2α (−/−) mice (Figure 4D–E). This was consistent with the reduced neutrophil recruitment observed in these mice. Monocyte-associated chemokines MCP-1 and MCP-5 were similarly reduced in HIF-2α (−/−) mice (Figure 4F–G). TGF-β levels were also lower in knockout mice at later time points after injury (Figure 4H). In contrast, BAL RAGE levels were transiently higher in HIF-2α (−/−) mice at 24 hours after contusion (Figure 4I). Together, these findings suggest that epithelial HIF-2α contributes to alveolar-capillary barrier dysfunction and inflammatory mediator production following lung contusion.

**Figure 5. HIF-2α regulates inflammatory and hypoxia-responsive gene expression following contusion**

To further examine the role of HIF-2α in lung inflammation after contusion, we measured gene expression in lungs from injured and uninjured HIF-2α (+/+) and HIF-2α (−/−) mice (n = 6 per group). Expression of the proinflammatory cytokines IL-1β, IL-6, and TNF-α increased in HIF-2α (+/+) mice following LC, with peak expression at 24 hours after injury (Figure 5A–C). These increases were significantly lower in HIF-2α (−/−) mice. We also examined caspase-1 (*Casp1*), which encodes a key protease involved in inflammasome signaling and IL-1β processing. *Casp1* expression increased progressively in HIF-2α (+/+) mice, reaching its highest level at 48 hours, whereas expression was lower in HIF-2α (−/−) mice (Figure 5D). These measurements reflect changes in *Casp1* transcript levels rather than caspase-1 activation, which was assessed separately in macrophages (Figure 8D–G).

We next examined the expression of hypoxia-responsive genes. VEGFA expression increased following contusion in HIF-2α (+/+) mice but was lower in HIF-2α (−/−) mice (Figure 5E). In contrast, FIZZ1 expression was higher in knockout mice, particularly at 24 hours after injury (Figure 5F). We also measured Glut-1 expression as a marker of the hypoxic response. Glut-1 expression was higher in HIF-2α (−/−) mice than in HIF-2α (+/+) mice at the time points examined, although expression declined over time in both groups (Figure 5G; n = 3 per group). Together, these findings suggest that HIF-2α contributes to the regulation of inflammatory and hypoxia-responsive gene expression following lung contusion.

**Figure 6. HIF-2α regulates NF-κB p65 expression following lung contusion**

Because NF-κB signaling is a central mediator of inflammatory lung injury (43, 44), we examined whether HIF-2α influences NF-κB p65 expression following LC. HIF-2α (+/+) and HIF-2α (−/−) mice were subjected to LC, and lung tissues were collected at 0, 24, and 48 hours after injury. HIF-2α expression increased in whole-lung tissue from HIF-2α (+/+) mice at 24 and 48 hours following contusion, whereas this increase was markedly attenuated in HIF-2α (−/−) mice (n = 6 per group) (Figure 6A). A similar pattern was observed in isolated type II alveolar epithelial cells (Figure 6B). Capillary Western blot analysis also showed increased HIF-2α protein expression in injured control lungs, with minimal expression in knockout mice (n = 3 per group) (Figure 6C–D).

We next examined NF-κB p65 expression following LC. In HIF-2α (+/+) mice, p65 expression increased after injury, reaching its highest level at 24 hours and remaining elevated at 48 hours (n = 6 per group) (Figure 6E). In contrast, p65 expression was substantially lower in HIF-2α (−/−) mice. Similar differences were observed in isolated type II alveolar epithelial cells, where p65 expression was higher in control mice than in knockout mice following injury (Figure 6F). Capillary Western blot analysis further confirmed increased p65 protein expression in injured control lungs, whereas expression remained low in HIF-2α (−/−) mice (n = 3 per group) (Figure 6G–H). Together, these findings suggest that HIF-2α contributes to increased NF-κB p65 expression following lung contusion.

**Figure 7. HIF signaling promotes inflammatory and metabolic responses in macrophages**

Because IL-1β was increased following lung contusion, we next examined whether HIF signaling influences inflammatory responses in macrophages. Bone marrow-derived macrophages (BMDMs) were treated with the HIF stabilizer FG-4592 or exposed to hypoxia, and inflammatory and hypoxia-responsive gene expression was measured.

FG-4592 treatment increased expression of IL-1β, IL-6, and IL-12 compared with control cells (n = 3 independent experiments) (Figure 7A–C). Hypoxia also increased cytokine expression, although the changes were generally less pronounced than those observed with FG-4592. Expression of the glycolytic marker PGK-1 increased under both conditions (Figure 7D). VEGFA expression was also increased following FG-4592 treatment and hypoxic exposure (Figure 7E). Among the chemokines examined, CXCL2 expression increased significantly with FG-4592 treatment, whereas hypoxia produced a more modest increase (Figure 7F). In contrast, CCL2 expression decreased following FG-4592 treatment but increased under hypoxic conditions (Figure 7G). TNFα expression showed little change across the treatment groups (Figure 7H).

We performed similar experiments in RAW264.7 macrophages. FG-4592 strongly increased IL-1β expression, whereas hypoxia produced a more modest increase (n = 3 independent experiments) (Figure 7I). CXCL2 expression was also markedly increased following FG-4592 treatment and modestly increased under hypoxic conditions (Figure 7J). CCL2 expression did not differ significantly among the groups (Figure 7K). GLUT1 expression increased substantially following FG-4592 treatment and remained elevated under hypoxic conditions (Figure 7L). VEGFA expression showed a similar pattern (Figure 7M). TNFα expression varied only modestly among the groups and was reduced under hypoxic conditions (Figure 7N).

Together, these findings show that pharmacological HIF stabilization and hypoxia produce distinct inflammatory and metabolic gene expression responses in macrophages.

**Figure 8. HIF-2α regulates IL-1β transcription and inflammasome activation in macrophages**

To determine whether HIF signaling regulates IL-1β transcription, macrophages were transfected with an IL-1β promoter luciferase reporter together with HIF-1α or HIF-2α expression vectors. HIF-2α markedly increased IL-1β promoter activity compared with HIF-1α. Mutation of the hypoxia-response elements (HREs) within the IL-1β promoter abolished HIF-dependent transcriptional activation, indicating that this response requires intact HREs (n = 3 independent experiments) (Figure 8A). Pharmacological inhibition of HIF-2α with PT2385 significantly reduced HIF-2α-induced IL-1β promoter activity (Figure 8B). To further examine the selectivity of PT2385, we measured enolase (p2.1) promoter activity. Both HIF-1α and HIF-2α increased enolase promoter activity; however, PT2385 selectively inhibited HIF-2α-dependent transcription without significantly affecting HIF-1α-mediated activation (Figure 8C). These findings support the selectivity of PT2385 for HIF-2α under the conditions tested.

Because IL-1β maturation requires inflammasome-mediated caspase-1 activation, we next examined the effects of HIF signaling on caspase-1 cleavage. Treatment with the HIF stabilizer FG-4592 increased cleavage of caspase-1 to its active p20 subunit, whereas PT2385 markedly reduced caspase-1 cleavage (Figure 8D–E). Similar findings were observed under hypoxic conditions, where PT2385 significantly attenuated hypoxia-induced caspase-1 activation compared with vehicle-treated controls (n = 3 independent experiments) (Figure 8F–G).

Finally, co-immunoprecipitation analysis demonstrated an association between HIF-2α and NLRP3 (Figure 8H). This finding suggests a potential link between HIF-2α and NLRP3

inflammasome signaling. Together, these findings indicate that HIF-2α promotes IL-1β transcription and contributes to caspase-1 activation in macrophages. Pharmacological inhibition of HIF-2α with PT2385 attenuates these responses.

**Figure 9A. HIF-2α deficiency protects against lethal *Klebsiella pneumoniae* infection**

To investigate the role of HIF-2α in infectious lung injury, C57BL/6, HIF-2α (+/+), and HIF-2α (−/−) mice were challenged with a lethal dose of *Klebsiella pneumoniae* in an independent infection model without prior lung contusion. C57BL/6 and HIF-2α (+/+) mice exhibited progressive mortality following infection, whereas HIF-2α (−/−) mice showed significantly improved survival (n = 8 animals per group) (Figure 9A). The survival difference between HIF-2α (+/+) and HIF-2α (−/−) mice was evident early after infection and persisted throughout the observation period. These findings indicate that HIF-2α deficiency is associated with improved survival following severe *K. pneumoniae* infection.

**Figure 9B. Pulmonary contusion induces regional histologic lung injury in a porcine model**

Histological examination of porcine lungs 1 hour after pulmonary contusion revealed differences in injury severity across the sampled lung regions. Contralateral lung tissue showed relatively preserved alveolar architecture with minimal inflammatory cell infiltration. Adjacent ipsilateral non-contused lung tissue exhibited mild to moderate septal thickening and inflammatory cell accumulation. The contused region showed the most severe injury, characterized by marked inflammatory cell infiltration, alveolar wall thickening, and disruption of normal alveolar architecture (n = 4 animals) (Figure 9B–C). Consistent with these findings, histopathological injury scores were significantly higher in the contused region than in the adjacent ipsilateral and contralateral lung regions.

**Figure 9C. HIF-2α expression is increased in injured porcine lung tissue**

To examine HIF-2α expression in a large-animal model of lung injury, HIF-2α protein levels were assessed in porcine lung tissue by capillary Western blot analysis. HIF-2α expression was similar in contralateral and adjacent ipsilateral non-contused lung regions. In contrast, the contused lung region showed a marked increase in HIF-2α protein abundance, with densitometric analysis demonstrating an approximately twofold increase compared with the contralateral region (n = 4 animals) (Figure 9C–D). These findings demonstrate increased HIF-2α expression in the injured lung region and are consistent with the findings from the murine model.

**Figure 10. HIF-2α links hypoxic stress to NF-κB–NLRP3–dependent inflammatory signaling in human and experimental lung contusion**

Human lung specimens and single-cell transcriptomic analyses show increased HIF-2α expression and EPAS1 transcripts, respectively, in alveolar epithelial cells and macrophage populations following lung injury. In experimental lung contusion, epithelial cell-specific HIF-2α deficiency reduces inflammatory mediator production, alveolar-capillary barrier injury, and pulmonary dysfunction. HIF-2α deficiency is also associated with reduced NF-κB p65 expression in injured lungs. In cultured macrophages, HIF signaling promotes IL-1β transcription and caspase-1 cleavage, while co-immunoprecipitation demonstrates an association between HIF-2α and NLRP3. Together, these findings support a proposed role for HIF-2α in regulating inflammatory responses following lung contusion through epithelial and macrophage-associated pathways.

**Discussion**

Lung contusion (LC) is a major risk factor for acute respiratory distress syndrome (ARDS) following blunt thoracic trauma. Although tissue hypoxia is a defining feature of LC, the mechanisms linking hypoxic stress to persistent inflammation and lung injury remain incompletely understood. In the present study, we identify HIF-2α as a central regulator of post-traumatic inflammatory lung injury. Using human lung specimens, single-cell transcriptomic analyses, conditional epithelial HIF-2α knockout mice, and complementary macrophage studies, we demonstrate that HIF-2α promotes NF-κB and NLRP3 signaling, enhances inflammatory cytokine production, and contributes to permeability injury following LC. Furthermore, genetic deletion or pharmacologic inhibition of HIF-2α attenuated inflammatory responses and improved survival following severe bacterial pneumonia. Together, these findings identify HIF-2α as an important link between hypoxic stress and inflammatory signaling in acute lung injury.

HIF-2α expression increased in human, porcine, and murine lungs after LC, supporting a conserved role for HIF-2α in hypoxia-associated lung injury. These findings are consistent with previous studies demonstrating distinct regulatory functions of HIF-2α in pulmonary inflammation and epithelial injury (45, 46). Published single-cell sequencing data from patients with severe ARDS further support increased HIF-2α expression in alveolar epithelial cells and macrophages during persistent lung injury (47). Importantly, our findings extend these observations by demonstrating a functional role for HIF-2α in regulating permeability injury and inflammatory signaling after trauma. Epithelial-specific deletion of HIF-2α reduced alveolar-capillary barrier

dysfunction, preserved lung compliance, and attenuated inflammatory cytokine and chemokine production following LC, indicating that epithelial HIF-2α contributes directly to the propagation of lung injury.

Neutrophil recruitment was also significantly reduced in HIF-2α–deficient mice. Neutrophils are key mediators of tissue damage following LC and contribute to disruption of the alveolar-capillary barrier through release of proteases, reactive oxygen species, and inflammatory mediators (31, 39). The reduction in neutrophil accumulation observed in HIF-2α–deficient mice were accompanied by lower levels of KC and MIP-2, suggesting that HIF-2α promotes recruitment of inflammatory cells into the injured lung. Mechanistically, loss of HIF-2α was associated with diminished NF-κB activation following injury, supporting HIF-2α as an upstream regulator of NF-κB–dependent inflammatory signaling. Crosstalk between hypoxia-responsive pathways and NF-κB has been reported in several inflammatory diseases (44, 48, 49), and our findings support a similar interaction during traumatic lung injury.

In addition to its effects in epithelial cells, HIF-2α played an important role in regulating macrophage inflammatory responses. Both hypoxia and pharmacologic activation of HIF signaling increased expression of inflammatory cytokines and hypoxia-responsive genes in macrophages. Notably, HIF-2α enhanced IL-1β promoter activity through functional hypoxia-responsive elements, supporting direct transcriptional regulation of IL-1β. These findings extend previous studies linking HIF signaling to macrophage activation and inflammatory cytokine production (39, 50). However, the effects of HIF-2α on inflammation may vary depending on the cellular and disease context. For example, HIF-2α signaling in liver macrophages has been shown to protect against acute liver injury through IL-6 production (51). Studies of remote ischemic preconditioning have also linked HIF signaling to reduced inflammatory responses, although the specific contribution of HIF-2α remains unclear (52). These findings highlight the context-dependent effects of HIF-2α in inflammatory diseases. In traumatic lung injury, our results support a proinflammatory role for HIF-2α, potentially involving NF-κB signaling and increased inflammatory cytokine production. Given that IL-1β is a major mediator of acute lung injury and ARDS, the regulation of IL-1β transcription by HIF-2α may represent an important mechanism through which hypoxia amplifies inflammatory responses following trauma.

A particularly important finding of the present study is the relationship between HIF-2α and inflammasome activation. NLRP3 inflammasome signaling is increasingly recognized as a critical

contributor to sterile lung inflammation and ARDS (53, 54). We found that HIF-2α deficiency reduced caspase-1 expression in vivo, while pharmacologic inhibition of HIF-2α attenuated caspase-1 activation in macrophages. In addition, co-immunoprecipitation studies demonstrated an interaction between HIF-2α and NLRP3, supporting a mechanistic connection between hypoxia signaling and inflammasome activation. Although additional studies will be required to define the precise molecular basis of this interaction, our findings suggest that HIF-2α regulates both transcriptional and post-translational pathways involved in IL-1β production. These observations position HIF-2α upstream of key inflammatory pathways that drive tissue injury after LC.

The therapeutic implications of these findings are noteworthy. Pharmacologic inhibition of HIF-2α with PT2385 significantly reduced IL-1β promoter activity and inflammasome activation in macrophages, supporting the concept that HIF-2α represents a druggable target in acute lung injury. Notably, PT2385, a selective HIF-2α inhibitor, has demonstrated efficacy in both preclinical models and clinical studies of HIF-2α–dependent diseases, further highlighting the translational potential of targeting HIF-2α–mediated inflammatory pathways (42, 55). Although our experiments were limited to in vitro studies, these findings raise the possibility that targeting HIF-2α could attenuate excessive inflammatory responses following trauma and reduce progression to ARDS.

An additional finding was the marked survival advantage observed in HIF-2α–deficient mice following lethal Klebsiella pneumoniae infection. While the mechanisms responsible for this protection remain to be fully defined, these results suggest that the proinflammatory effects of HIF-2α extend beyond sterile injury and may contribute to the pathogenesis of severe bacterial pneumonia. Reduced NF-κB activation, diminished inflammasome signaling, and lower cytokine production may collectively limit excessive host inflammatory responses during infection. These findings further support the concept that HIF-2α functions as a central regulator of inflammatory lung injury under both sterile and infectious conditions.

**Limitations**

Several limitations should be considered. First, the present study focused on the acute inflammatory response following lung contusion; therefore, the role of HIF-2α in subsequent lung repair and remodeling remains unclear. Although our findings suggest a relationship between HIF-2α, NF-κB, and NLRP3 signaling, the underlying molecular mechanisms, particularly the relationship between epithelial HIF-2α and macrophage responses in vivo, require further

investigation. Second, formal randomization was not performed in the mouse experiments, although histological assessments were conducted by an investigator blinded to genotype and injury condition. The pressure–volume measurements also do not directly assess respiratory-system resistance or tissue mechanics. In addition, the porcine model combined hemorrhagic shock and pulmonary contusion without separate injury controls and included only a single early time point (1 hour), limiting the interpretation of the individual contributions of each injury.

Third, the *K. pneumoniae* experiment was conducted as an independent model of infectious lung injury, not as a post-traumatic second-hit model. Although HIF-2α deficiency improved survival, bacterial burden was not measured. Therefore, these findings do not establish a direct link between traumatic lung injury and subsequent infection. Finally, the human postmortem specimens were limited to three patients, and clinical factors such as mechanical ventilation, infection, systemic inflammation, and postmortem interval could not be fully controlled. Larger, clinically characterized human cohorts and further mechanistic studies are needed to validate these findings and better define the role of HIF-2α in lung injury and repair.

**Conclusion**

Our findings identify HIF-2α as an important regulator of the acute inflammatory response following lung contusion. In the mouse model, type II alveolar epithelial cell-specific HIF-2α deficiency attenuated inflammatory mediator production, alveolar-capillary barrier injury, and pulmonary dysfunction. In cultured macrophages, HIF signaling promoted IL-1β transcription and caspase-1 activation, while co-immunoprecipitation demonstrated an association between HIF-2α and NLRP3. HIF-2α deficiency was also associated with improved survival following severe *Klebsiella pneumoniae* infection in an independent infectious lung injury model. Collectively, these findings support further investigation of HIF-2α as a potential therapeutic target in acute lung injury and ARDS.

**Figure legends**

**Figure 1. HIF-2α is increased in human and experimental lung contusion**

Postmortem human lung specimens from patients with lung contusion (LC) and uninjured controls were examined for HIF-2α expression. Immunohistochemical staining showed increased HIF-2α expression in contused lungs, particularly in the alveolar epithelium (A), with quantification of DAB staining intensity shown in (B). Immunofluorescence staining further confirmed increased HIF-2α expression in contused lungs compared with uninjured controls (C), with quantification

shown in (D). Human specimens were limited to three patients per group.Human specimens were limited to three patients per group. Single-cell RNA-sequencing data from McCall et al. (23) showed increased EPAS1 expression in epithelial cells and macrophage populations associated with lung injury (E). In mice, immunofluorescence staining showed increased HIF-2α expression following LC in HIF-2α (+/+) lungs, whereas staining was markedly reduced in HIF-2α (−/−) lungs (F), with quantification shown in (G) (n = 3 per group). Data are presented as mean ± SEM. Comparisons between two groups were performed using an unpaired, two-tailed Student's t-test with Welch's correction. $P < 0.05$.

**Figure 2. Generation and validation of epithelial HIF-2α–deficient mice**

Representative PCR genotyping of tail DNA showing the floxed HIF-2α allele (220 bp), Cre transgene (370 bp), and SP-C-rtTA transgene (350 bp) (A, B). Following doxycycline-induced recombination, quantitative PCR showed reduced *Epas1* mRNA expression in HIF-2α (−/−) lungs compared with HIF-2α (+/+) controls (C). Capillary Western blot analysis confirmed reduced HIF-2α protein expression in HIF-2α (−/−) lungs, with GAPDH used as the loading control (D). The blot is representative of three mice per genotype. Immunofluorescence staining of uninjured lungs showed HIF-2α expression in the alveolar epithelium of HIF-2α (+/+) mice, with weaker staining in HIF-2α (−/−) mice (DAPI, blue; HIF-2α, red) (E). Scale bar, 50 μm. Data are presented as mean ± SEM. Genotype comparisons were performed using an unpaired, two-tailed Student's *t*-test. $P < 0.05$.

**Figure 3. Epithelial HIF-2α deletion reduces lung injury following contusion**

Pressure–volume measurements were obtained at 24 and 48 hours after lung contusion (LC). HIF-2α (+/+) mice showed altered pressure–volume responses following injury, whereas these changes were less pronounced in HIF-2α (−/−) mice (A; n = 6 per group). These measurements reflect the overall pressure–volume response and do not directly measure respiratory-system resistance or tissue mechanics. Representative H&E-stained lung sections showed more severe injury in HIF-2α (+/+) mice, characterized by alveolar hemorrhage, inflammatory cell infiltration, and disruption of alveolar architecture. These changes were less pronounced in HIF-2α (−/−) mice (B; n = 3 per group). Histological scoring was performed by an investigator blinded to genotype and injury condition. Injury scores are presented as median (IQR and range) and were analyzed using the Kruskal–Wallis test followed by Dunn's multiple-comparisons test. Bronchoalveolar lavage fluid (BALF) differential cell counts showed increased neutrophil numbers in HIF-2α (+/+) mice

compared with HIF-2α (−/−) mice, whereas macrophage numbers did not differ significantly between genotypes (C; n = 3 per group). $P < 0.05$.

**Figure 4. Epithelial HIF-2α deletion reduces permeability injury and inflammation after contusion**

Bronchoalveolar lavage (BAL) fluid was collected at 0, 5, 24, 48, and 72 hours after lung contusion (LC), using separate animals at each time point. BAL albumin levels increased after injury and were higher in HIF-2α (+/+) mice than in HIF-2α (−/−) mice at 5, 24, and 48 hours. This difference was no longer evident at 72 hours (A; n = 10 per group). BAL levels of IL-6, TNF-α, macrophage inflammatory protein-2 (MIP-2/CXCL2), and keratinocyte chemoattractant (KC/CXCL1) were also higher in HIF-2α (+/+) mice, particularly at earlier time points (B–E). Monocyte-associated chemokines MCP-1 and MCP-5 were higher in HIF-2α (+/+) mice (F, G). TGF-β levels were lower in HIF-2α (−/−) mice at later time points (H). In contrast, BAL RAGE levels were transiently higher in HIF-2α (−/−) mice at 24 hours after injury (I). Data are presented as mean ± SEM and were analyzed using two-way ANOVA followed by Tukey's multiple-comparisons test. $P < 0.05$.

**Figure 5. HIF-2α deletion reduces inflammatory and hypoxia-responsive gene expression after contusion**

Gene expression was measured in whole-lung tissue from HIF-2α (+/+) and HIF-2α (−/−) mice at 0, 24, and 48 hours after lung contusion (LC). IL-1β, IL-6, and TNF-α expression increased after LC in HIF-2α (+/+) mice and was lower in HIF-2α (−/−) mice (A–C; n = 6 per group). *Casp1* expression also increased over time in HIF-2α (+/+) mice but remained lower in HIF-2α (−/−) mice (D; n = 6 per group). These results reflect *Casp1* transcript levels and do not indicate caspase-1 activation. VEGFA expression increased after injury in HIF-2α (+/+) mice and was lower in HIF-2α (−/−) mice (E). FIZZ1 expression was higher in HIF-2α (−/−) mice, particularly at 24 hours (F; n = 6 per group). Glut-1 expression was higher in HIF-2α (−/−) mice and declined over time in both genotypes (G; n = 3 per group). Data are presented as mean ± SEM. Comparisons between two groups at individual time points were performed using an unpaired, two-tailed Student's *t*-test with Welch's correction. $P < 0.05$.

**Figure 6. HIF-2α deletion reduces NF-κB p65 expression after lung contusion**

HIF-2α and NF-κB p65 expression were examined in whole-lung tissue and isolated type II alveolar epithelial cells following lung contusion (LC). HIF-2α expression increased after injury in HIF-2α (+/+) mice but remained markedly lower in HIF-2α (−/−) mice in both whole-lung tissue

(A) and isolated type II alveolar epithelial cells (B; n = 6 per group). Capillary Western blot analysis confirmed increased HIF-2α protein expression in injured HIF-2α (+/+) lungs, with minimal expression in HIF-2α (−/−) lungs (C, D; n = 3 per group). NF-κB p65 expression also increased after LC in HIF-2α (+/+) mice, reaching its highest level at 24 hours and remaining elevated at 48 hours. Expression was lower in HIF-2α (−/−) mice (E, F; n = 6 per group). Capillary Western blot analysis further confirmed these differences at the protein level (G, H; n = 3 per group). Data are presented as mean ± SEM and were analyzed using two-way ANOVA, with genotype and time as factors, followed by Tukey's multiple-comparisons test. $P < 0.05$.

**Figure 7. HIF signaling promotes inflammatory and metabolic gene expression in macrophages in vitro**

Bone marrow-derived macrophages (BMDMs) and RAW264.7 cells were treated with the HIF stabilizer FG-4592 (10 μM) or exposed to hypoxia (1% $O_2$) for 16 hours. In BMDMs, both FG-4592 treatment and hypoxia increased the expression of IL-1β, IL-6, IL-12, PGK-1, VEGFA, and CXCL2 (A–F). CCL2 expression decreased after FG-4592 treatment but increased under hypoxic conditions, while TNF-α expression changed little across the treatment groups (G, H). In RAW264.7 cells, FG-4592 treatment and hypoxia increased the expression of IL-1β, CXCL2, GLUT1, and VEGFA (I, J, L, M). CCL2 expression did not differ significantly among the groups, while TNF-α expression showed modest changes and was lower under hypoxic conditions (K, N). Gene expression was normalized to housekeeping genes and expressed as fold change relative to untreated controls. Data are from three independent experiments and are presented as mean ± SEM. Comparisons were performed using one-way ANOVA followed by Tukey's multiple-comparisons test. $P < 0.05$.

**Figure 8. HIF-2α regulates IL-1β transcription and caspase-1 activation in macrophages in**

Luciferase reporter assays showed that HIF-2α increased IL-1β promoter activity more than HIF-1α. Mutation of hypoxia-response elements (HREs) in the IL-1β promoter abolished HIF-dependent activation (A). PT2385 (10 μM) reduced HIF-2α-induced IL-1β promoter activity (B). Both HIF-1α and HIF-2α increased enolase (p2.1) promoter activity, whereas PT2385 selectively reduced the HIF-2α-dependent response without significantly affecting HIF-1α-mediated activation (C). Western blot analysis showed increased caspase-1 cleavage, indicated by the p20 subunit, following FG-4592 treatment. This response was reduced by PT2385 under normoxic conditions (D, E) and following hypoxia exposure (F, G). Co-immunoprecipitation demonstrated

an association between HIF-2α and NLRP3 (H). PT2385 was used only in these in vitro experiments and was not administered to animals. Data are presented as mean ± SEM from three independent experiments. Statistical comparisons were performed using one-way ANOVA followed by Tukey's multiple-comparisons test. $P < 0.05$.

**Figure 9. Survival, regional lung injury, and HIF-2α expression in experimental infection and porcine lung injury models**

Kaplan–Meier survival curves of C57BL/6 HIF-2α (+/+) and HIF-2α (−/−) mice following oropharyngeal aspiration of 500 CFU of *Klebsiella pneumoniae*. Survival was monitored for 10 days (n = 8 per group). HIF-2α (−/−) mice showed improved survival compared with HIF-2α (+/+) mice. Bacterial burden was not measured. This was an independent infection model without prior lung contusion. Survival was compared using the log-rank (Mantel–Cox) test. $P < 0.05$ (A).

Representative H&E-stained lung sections (B) and histological injury scores (C) from contralateral, adjacent ipsilateral non-contused, and contused lung regions of Yorkshire swine subjected to pulmonary contusion and controlled hemorrhage (40% blood volume) and euthanized 1 hour after injury. The contused region showed greater histological injury than the other two regions. Original magnification, ×20; scale bar, 50 μm. Injury scores were assessed by a blinded investigator and are presented as median (B, C). (IQR and range; n = 4 animals). Regional comparisons were performed using the Friedman test followed by Dunn's multiple-comparisons test. $P < 0.05$ versus contralateral lung

**Figure 10. Proposed model linking HIF-2α to inflammatory lung injury following lung contusion**

Schematic illustrating the proposed role of HIF-2α in inflammatory responses following lung contusion. Human lung specimens, single-cell transcriptomic analyses, and a porcine model of combined hemorrhagic shock and pulmonary contusion showed increased HIF-2α expression or *EPAS1* transcripts in injured lung tissue and relevant cell populations. In experimental lung contusion, type II alveolar epithelial cell-specific HIF-2α deficiency reduced inflammatory mediator production, alveolar-capillary barrier injury, and pulmonary dysfunction. HIF-2α deficiency was also associated with reduced NF-κB p65 expression in injured lungs. In cultured macrophages, HIF signaling promoted IL-1β transcription and caspase-1 cleavage, while co-immunoprecipitation demonstrated an association between HIF-2α and NLRP3. Together, these

findings support a proposed role for HIF-2α in regulating inflammatory responses through epithelial and macrophage-associated pathways.

**Author Contributions**

MVS contributed to the study conception and design, investigation, project administration, supervision, validation, visualization, data curation, methodology, formal analysis, and manuscript drafting, review, and editing. SS contributed to investigation, data curation, and manuscript review and editing. NB and CC contributed to data curation. NK, AB, BM, and YMS contributed to manuscript review and editing. KR contributed to supervision, validation, visualization, funding acquisition, resources, and manuscript review and editing. All authors reviewed and approved the final manuscript.

**Acknowledgments**

This work was supported by the National Institutes of Health Grant HL102013 (to KR). The opinions and assertions expressed herein are those of the author(s) and do not reflect the official policy or position of the Uniformed Services University of the Health Sciences or the Department of War.

**Conflict of Interest Statement**

The authors declare that they have no competing interests.

**Data Availability Statement**

The data that support the findings of this study are available from the corresponding author upon reasonable request.

**References**

1. Knoferl MW, Liener UC, Perl M, Bruckner UB, Kinzl L, and Gebhard F. Blunt chest trauma induces delayed splenic immunosuppression. *Shock.* 2004;22(1):51-6.
2. Wang ND, Stevens MH, Doty DB, and Hammond EH. Blunt chest trauma: an experimental model for heart and lung contusion. *J Trauma.* 2003;54(4):744-8.
3. ARDS_Network. Ventilation with lower tidal volumes as compared with traditional tidal volumes for acute lung injury and the acute respiratory distress syndrome. The Acute Respiratory Distress Syndrome Network. *N Engl J Med.* 2000;342:1301-8.
4. Control CfD. Morbidity and Mortality weekly report. 1997;46(RR-1):1-79.
5. Rosseau S, and Suttorp N. [Community-acquired infections of the respiratory tract and lung parenchyma. Clinical and experimental aspects]. *Internist (Berl).* 2000;41(11):1158, 61-9.
6. Miller PR, Croce MA, Bee TK, Qaisi WG, Smith CP, Collins GL, et al. ARDS after pulmonary contusion: accurate measurement of contusion volume identifies high-risk patients. *J Trauma.* 2001;51(2):223-8; discussion 9-30.

7. Hudson LD, Milberg JA, Anardi D, and Maunder RJ. Clinical risks for development of the acute respiratory distress syndrome. *Am J Respir Crit Care Med.* 1995;151(2 Pt 1):293-301.
8. Bauer TT, Ferrer R, Angrill J, Schultze-Werninghaus G, and Torres A. Ventilator-associated pneumonia: incidence, risk factors, and microbiology. *Semin Respir Infect.* 2000;15:272-9.
9. Iregui M, Ward S, Sherman G, Fraser VJ, and Kollef MH. Clinical importance of delays in the initiation of appropriate antibiotic treatment for ventilator-associated pneumonia. *Chest.* 2002;122(1):262-8.
10. Marik PE, and Careau P. The role of anaerobes in patients with ventilator-associated pneumonia and aspiration pneumonia: a prospective study. *Chest.* 1999;115(1):178-83.
11. Raghavendran K, Pryhuber GS, Chess PR, Davidson BA, Knight PR, and Notter RH. Pharmacotherapy of acute lung injury and acute respiratory distress syndrome. *Curr Med Chem.* 2008;15(19):1911-24.
12. Guo WA, Knight PR, and Raghavendran K. The receptor for advanced glycation end products and acute lung injury/acute respiratory distress syndrome. *Intensive Care Med.* 2012;38(10):1588-98.
13. Wang GL, Jiang BH, Rue EA, and Semenza GL. Hypoxia-inducible factor 1 is a basic-helix-loop-helix-PAS heterodimer regulated by cellular O2 tension. *Proc Natl Acad Sci U S A.* 1995;92(12):5510-4.
14. Jaakkola P, Mole DR, Tian YM, Wilson MI, Gielbert J, Gaskell SJ, et al. Targeting of HIF-alpha to the von Hippel-Lindau ubiquitylation complex by O2-regulated prolyl hydroxylation. *Science.* 2001;292(5516):468-72.
15. Maxwell PH, Wiesener MS, Chang GW, Clifford SC, Vaux EC, Cockman ME, et al. The tumour suppressor protein VHL targets hypoxia-inducible factors for oxygen-dependent proteolysis. *Nature.* 1999;399(6733):271-5.
16. Ema M, Taya S, Yokotani N, Sogawa K, Matsuda Y, and Fujii-Kuriyama Y. A novel bHLH-PAS factor with close sequence similarity to hypoxia-inducible factor 1alpha regulates the VEGF expression and is potentially involved in lung and vascular development. *Proc Natl Acad Sci U S A.* 1997;94(9):4273-8.
17. Compernolle V, Brusselmans K, Acker T, Hoet P, Tjwa M, Beck H, et al. Loss of HIF-2alpha and inhibition of VEGF impair fetal lung maturation, whereas treatment with VEGF prevents fatal respiratory distress in premature mice. *Nat Med.* 2002;8(7):702-10.
18. Wiesener MS, Jurgensen JS, Rosenberger C, Scholze CK, Horstrup JH, Warnecke C, et al. Widespread hypoxia-inducible expression of HIF-2alpha in distinct cell populations of different organs. *FASEB J.* 2003;17(2):271-3.
19. D'Ignazio L, Bandarra D, and Rocha S. NF-kappaB and HIF crosstalk in immune responses. *FEBS J.* 2016;283(3):413-24.
20. D'Ignazio L, and Rocha S. Hypoxia Induced NF-kappaB. *Cells.* 2016;5(1).
21. Chavez JC, Baranova O, Lin J, and Pichiule P. The transcriptional activator hypoxia inducible factor 2 (HIF-2/EPAS-1) regulates the oxygen-dependent expression of erythropoietin in cortical astrocytes. *J Neurosci.* 2006;26(37):9471-81.
22. Ivan M, Kondo K, Yang H, Kim W, Valiando J, Ohh M, et al. HIFalpha targeted for VHL-mediated destruction by proline hydroxylation: implications for O2 sensing. *Science.* 2001;292(5516):464-8.

23. McCall AS, Gutor S, Tanjore H, Burman A, Sherrill T, Chapman M, et al. Hypoxia-inducible factor 2 regulates alveolar regeneration after repetitive injury in three-dimensional cellular and in vivo models. *Sci Transl Med.* 2025;17(780):eadk8623.
24. Hu CJ, Poth JM, Zhang H, Flockton A, Laux A, Kumar S, et al. Suppression of HIF2 signalling attenuates the initiation of hypoxia-induced pulmonary hypertension. *Eur Respir J.* 2019;54(6).
25. Niu Y, Bao L, Chen Y, Wang C, Luo M, Zhang B, et al. HIF2-Induced Long Noncoding RNA RAB11B-AS1 Promotes Hypoxia-Mediated Angiogenesis and Breast Cancer Metastasis. *Cancer Res.* 2020;80(5):964-75.
26. Prabhakar NR, Peng YJ, and Nanduri J. Hypoxia-inducible factors and obstructive sleep apnea. *J Clin Invest.* 2020;130(10):5042-51.
27. Daly M, Miller PR, Carr JJ, Gayzik FS, Hoth JJ, Meredith JW, et al. Traumatic pulmonary pathology measured with computed tomography and a semiautomated analytic method. *Clin Imaging.* 2008;32(5):346-54.
28. Hoth JJ, Hudson WP, Brownlee NA, Yoza BK, Hiltbold EM, Meredith JW, et al. Toll-like receptor 2 participates in the response to lung injury in a murine model of pulmonary contusion. *Shock.* 2007;28(4):447-52.
29. Hoth JJ, Stitzel JD, Gayzik FS, Brownlee NA, Miller PR, Yoza BK, et al. The pathogenesis of pulmonary contusion: an open chest model in the rat. *J Trauma.* 2006;61(1):32-44; discussion -5.
30. Hoth JJ, Wells JD, Brownlee NA, Hiltbold EM, Meredith JW, McCall CE, et al. Toll-Like receptor 4 dependent responses to lung injury in a murine model of pulmonary contusion. *Shock.* 2008.
31. Suresh MV, Thomas B, Machado-Aranda D, Dolgachev VA, Kumar Ramakrishnan S, Talarico N, et al. Double-Stranded RNA Interacts With Toll-Like Receptor 3 in Driving the Acute Inflammatory Response Following Lung Contusion. *Crit Care Med.* 2016;44(11):e1054-e66.
32. Obertacke U, Neudeck F, Majetschak M, Hellinger A, Kleinschmidt C, Schade FU, et al. Local and systemic reactions after lung contusion: an experimental study in the pig. *Shock.* 1998;10(1):7-12.
33. Cohn SM, and Zieg PM. Experimental pulmonary contusion: review of the literature and description of a new porcine model. *J Trauma.* 1996;41(3):565-71.
34. Burmeister DM, McIntyre MK, Beely B, Jordan B, Walker KP, 3rd, Aden JK, et al. A model of recovery from inhalation injury and cutaneous burn in ambulatory swine. *Burns.* 2017;43(6):1295-305.
35. Zhang B, Swamy S, Balijepalli S, Panicker S, Mooliyil J, Sherman MA, et al. Direct pulmonary delivery of solubilized curcumin reduces severity of lethal pneumonia. *FASEB J.* 2019;33(12):13294-309.
36. Kim HC, Suresh MV, Singh VV, Arick DQ, Machado-Aranda DA, Raghavendran K, et al. Polymer Lung Surfactants. *ACS Appl Bio Mater.* 2018;1(3):581-92.
37. Suresh MV, Dolgachev VA, Zhang B, Balijepalli S, Swamy S, Mooliyil J, et al. TLR3 absence confers increased survival with improved macrophage activity against pneumonia. *JCI Insight.* 2019;4(23).
38. Silva IAN, Gvazava N, Bolukbas DA, Stenlo M, Dong J, Hyllen S, et al. A Semi-quantitative Scoring System for Green Histopathological Evaluation of Large Animal Models of Acute Lung Injury. *Bio Protoc.* 2022;12(16).

39. Suresh MV, Balijepalli S, Zhang B, Singh VV, Swamy S, Panicker S, et al. Hypoxia-Inducible Factor (HIF)-1alpha Promotes Inflammation and Injury Following Aspiration-Induced Lung Injury in Mice. *Shock.* 2019;52(6):612-21.
40. Fang HY, Hughes R, Murdoch C, Coffelt SB, Biswas SK, Harris AL, et al. Hypoxia-inducible factors 1 and 2 are important transcriptional effectors in primary macrophages experiencing hypoxia. *Blood.* 2009;114(4):844-59.
41. Li X, Zhang X, Xia J, Zhang L, Chen B, Lian G, et al. Macrophage HIF-2alpha suppresses NLRP3 inflammasome activation and alleviates insulin resistance. *Cell Rep.* 2021;36(8):109607.
42. Wallace EM, Rizzi JP, Han G, Wehn PM, Cao Z, Du X, et al. A Small-Molecule Antagonist of HIF2alpha Is Efficacious in Preclinical Models of Renal Cell Carcinoma. *Cancer Res.* 2016;76(18):5491-500.
43. Madjdpour L, Kneller S, Booy C, Pasch T, Schimmer RC, and Beck-Schimmer B. Acid-induced lung injury: role of nuclear factor-kappaB. *Anesthesiology.* 2003;99(6):1323-32.
44. Jung YJ, Isaacs JS, Lee S, Trepel J, and Neckers L. IL-1beta-mediated up-regulation of HIF-1alpha via an NFkappaB/COX-2 pathway identifies HIF-1 as a critical link between inflammation and oncogenesis. *FASEB J.* 2003;17(14):2115-7.
45. Proper SP, Saini Y, Greenwood KK, Bramble LA, Downing NJ, Harkema JR, et al. Loss of hypoxia-inducible factor 2 alpha in the lung alveolar epithelium of mice leads to enhanced eosinophilic inflammation in cobalt-induced lung injury. *Toxicol Sci.* 2014;137(2):447-57.
46. Geller E, Khaw BA, Strauss HW, Carvalho AC, Rajagopalan B, Jones R, et al. Technetium-fibrinogen lung scanning in canine lung contusion. *J Trauma.* 1984;24(7):611-8.
47. Bharat A, Querrey M, Markov NS, Kim S, Kurihara C, Garza-Castillon R, et al. Lung transplantation for patients with severe COVID-19. *Sci Transl Med.* 2020;12(574).
48. Palazon A, Goldrath AW, Nizet V, and Johnson RS. HIF transcription factors, inflammation, and immunity. *Immunity.* 2014;41(4):518-28.
49. Bauernfeind FG, Horvath G, Stutz A, Alnemri ES, MacDonald K, Speert D, et al. Cutting edge: NF-kappaB activating pattern recognition and cytokine receptors license NLRP3 inflammasome activation by regulating NLRP3 expression. *J Immunol.* 2009;183(2):787-91.
50. Suresh MV, Ramakrishnan SK, Thomas B, Machado-Aranda D, Bi Y, Talarico N, et al. Activation of hypoxia-inducible factor-1alpha in type 2 alveolar epithelial cell is a major driver of acute inflammation following lung contusion. *Crit Care Med.* 2014;42(10):e642-53.
51. Gao RY, Wang M, Liu Q, Feng D, Wen Y, Xia Y, et al. Hypoxia-Inducible Factor-2alpha Reprograms Liver Macrophages to Protect Against Acute Liver Injury Through the Production of Interleukin-6. *Hepatology.* 2020;71(6):2105-17.
52. Du X, Yang J, Liu C, Wang S, Zhang C, Zhao H, et al. Hypoxia-Inducible Factor 1alpha and 2alpha Have Beneficial Effects in Remote Ischemic Preconditioning Against Stroke by Modulating Inflammatory Responses in Aged Rats. *Front Aging Neurosci.* 2020;12:54.
53. Grailer JJ, Canning BA, Kalbitz M, Haggadone MD, Dhond RM, Andjelkovic AV, et al. Critical role for the NLRP3 inflammasome during acute lung injury. *J Immunol.* 2014;192(12):5974-83.

54. Dolinay T, Kim YS, Howrylak J, Hunninghake GM, An CH, Fredenburgh L, et al. Inflammasome-regulated cytokines are critical mediators of acute lung injury. *Am J Respir Crit Care Med.* 2012;185(11):1225-34.
55. Courtney KD, Infante JR, Lam ET, Figlin RA, Rini BI, Brugarolas J, et al. Phase I Dose-Escalation Trial of PT2385, a First-in-Class Hypoxia-Inducible Factor-2alpha Antagonist in Patients With Previously Treated Advanced Clear Cell Renal Cell Carcinoma. *J Clin Oncol.* 2018;36(9):867-74.

Figure 1

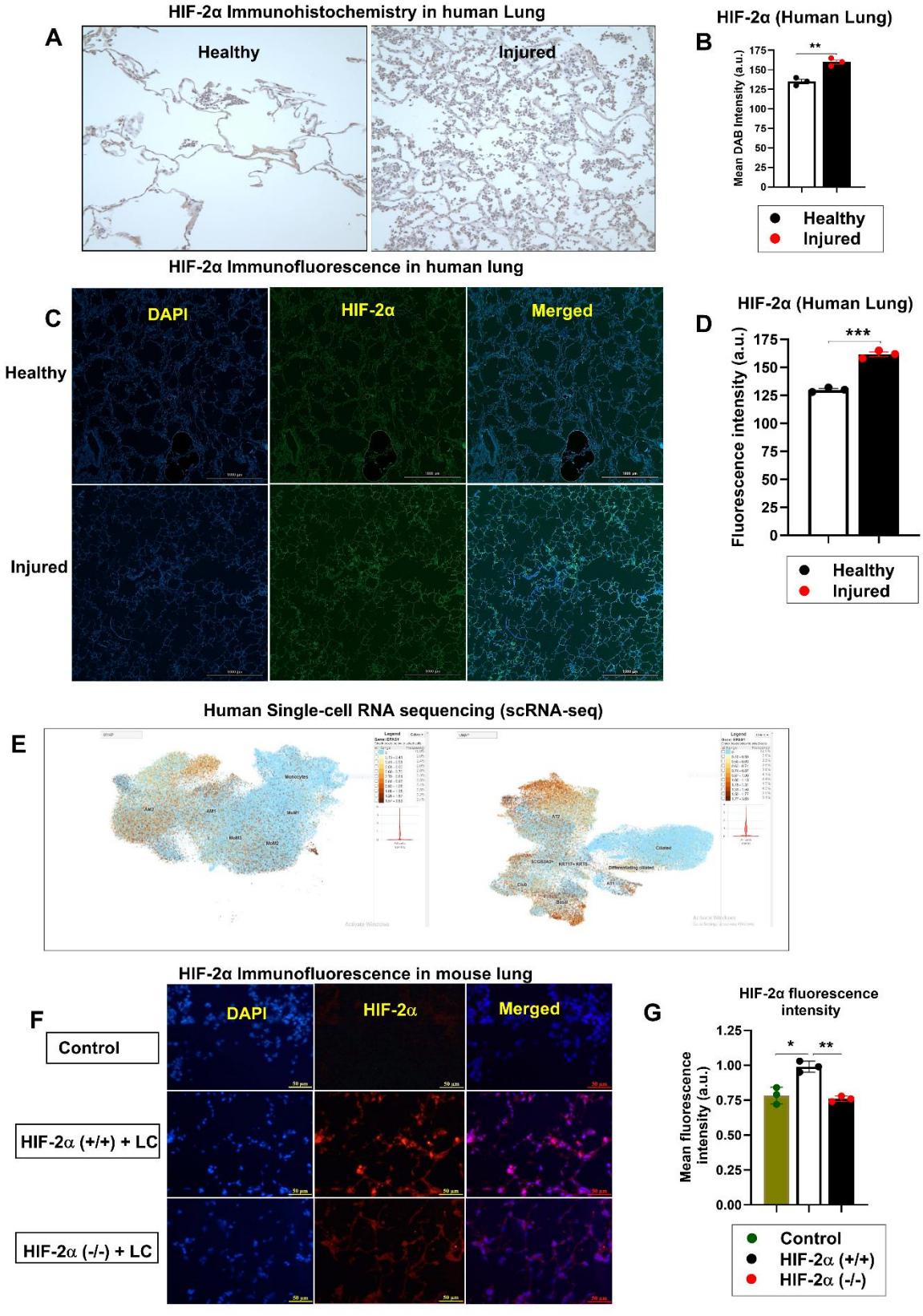

HIF-2α Immunohistochemistry in human Lung
A
Healthy
Injured
HIF-2α (Human Lung)
B
Mean DAB Intensity (a.u.)
Healthy
Injured
HIF-2α Immunofluorescence in human lung
C
DAPI
HIF-2α
Merged
Healthy
Injured
HIF-2α (Human Lung)
D
Fluorescence intensity (a.u.)
Healthy
Injured
Human Single-cell RNA sequencing (scRNA-seq)
E
HIF-2α Immunofluorescence in mouse lung
F
DAPI
HIF-2α
Merged
Control
HIF-2α (+/+) + LC
HIF-2α (-/-) + LC
HIF-2α fluorescence intensity
G
Mean fluorescence intensity (a.u.)
Control
HIF-2α (+/+)
HIF-2α (-/-)

**Figure 2**

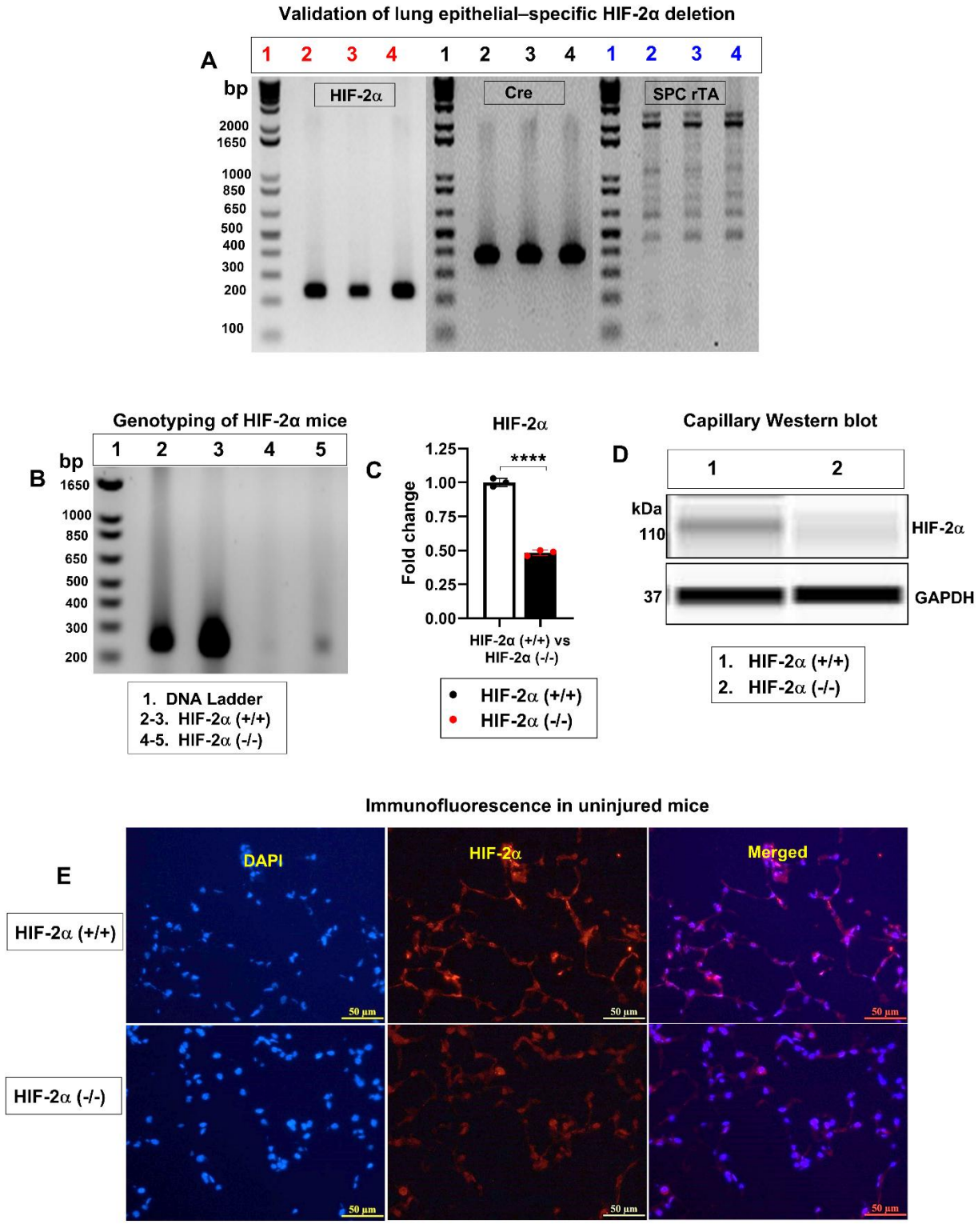

Validation of lung epithelial–specific HIF-2α deletion
A
1 2 3 4 1 2 3 4 1 2 3 4
bp
HIF-2α
Cre
SPC rTA
2000
1650
1000
850
650
500
400
300
200
100
Genotyping of HIF-2α mice
B
bp
1 2 3 4 5
1650
1000
850
650
500
400
300
200
1. DNA Ladder
2-3. HIF-2α (+/+)
4-5. HIF-2α (-/-)
HIF-2α
C
Fold change
1.25
1.00
0.75
0.50
0.25
0.00
****
HIF-2α (+/+) vs HIF-2α (-/-)
HIF-2α (+/+)
HIF-2α (-/-)
Capillary Western blot
D
1 2
kDa
110
HIF-2α
37
GAPDH
1. HIF-2α (+/+)
2. HIF-2α (-/-)
Immunofluorescence in uninjured mice
E
DAPI
HIF-2α
Merged
HIF-2α (+/+)
HIF-2α (-/-)
50 µm

**Figure 3**

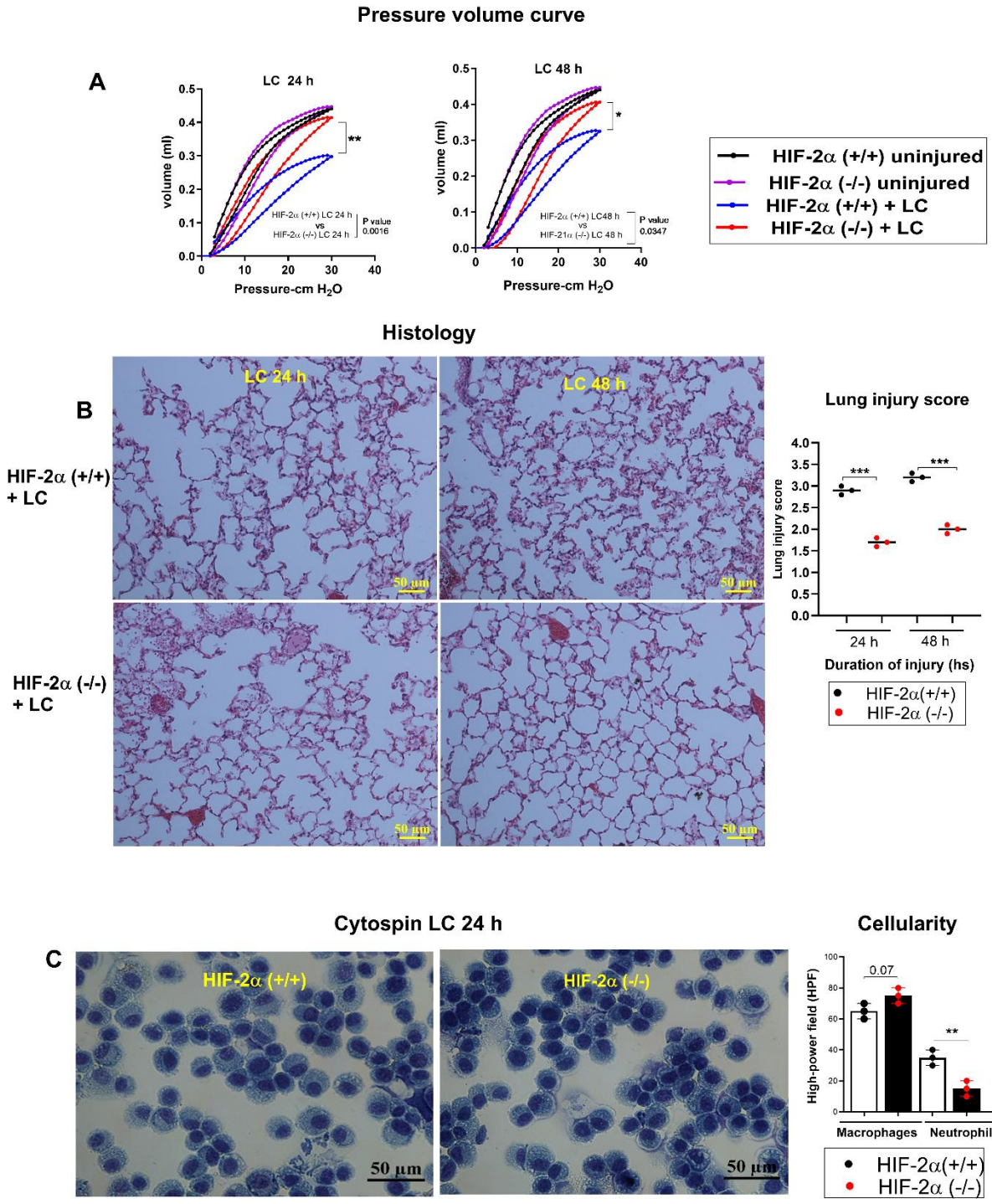

Pressure volume curve
A
LC 24 h
LC 48 h
volume (ml)
Pressure-cm H2O
HIF-2α (+/+) LC 24 h vs HIF-2α (-/-) LC 24 h
P value 0.0016
HIF-2α (+/+) LC48 h vs HIF-21α (-/-) LC 48 h
P value 0.0347
HIF-2α (+/+) uninjured
HIF-2α (-/-) uninjured
HIF-2α (+/+) + LC
HIF-2α (-/-) + LC
Histology
B
HIF-2α (+/+) + LC
HIF-2α (-/-) + LC
50 µm
Lung injury score
Lung injury score
24 h
48 h
Duration of injury (hs)
HIF-2α(+/+)
HIF-2α (-/-)
Cytospin LC 24 h
C
HIF-2α (+/+)
HIF-2α (-/-)
Cellularity
High-power field (HPF)
0.07
Macrophages
Neutrophils
HIF-2α(+/+)
HIF-2α (-/-)

**Figure 4**

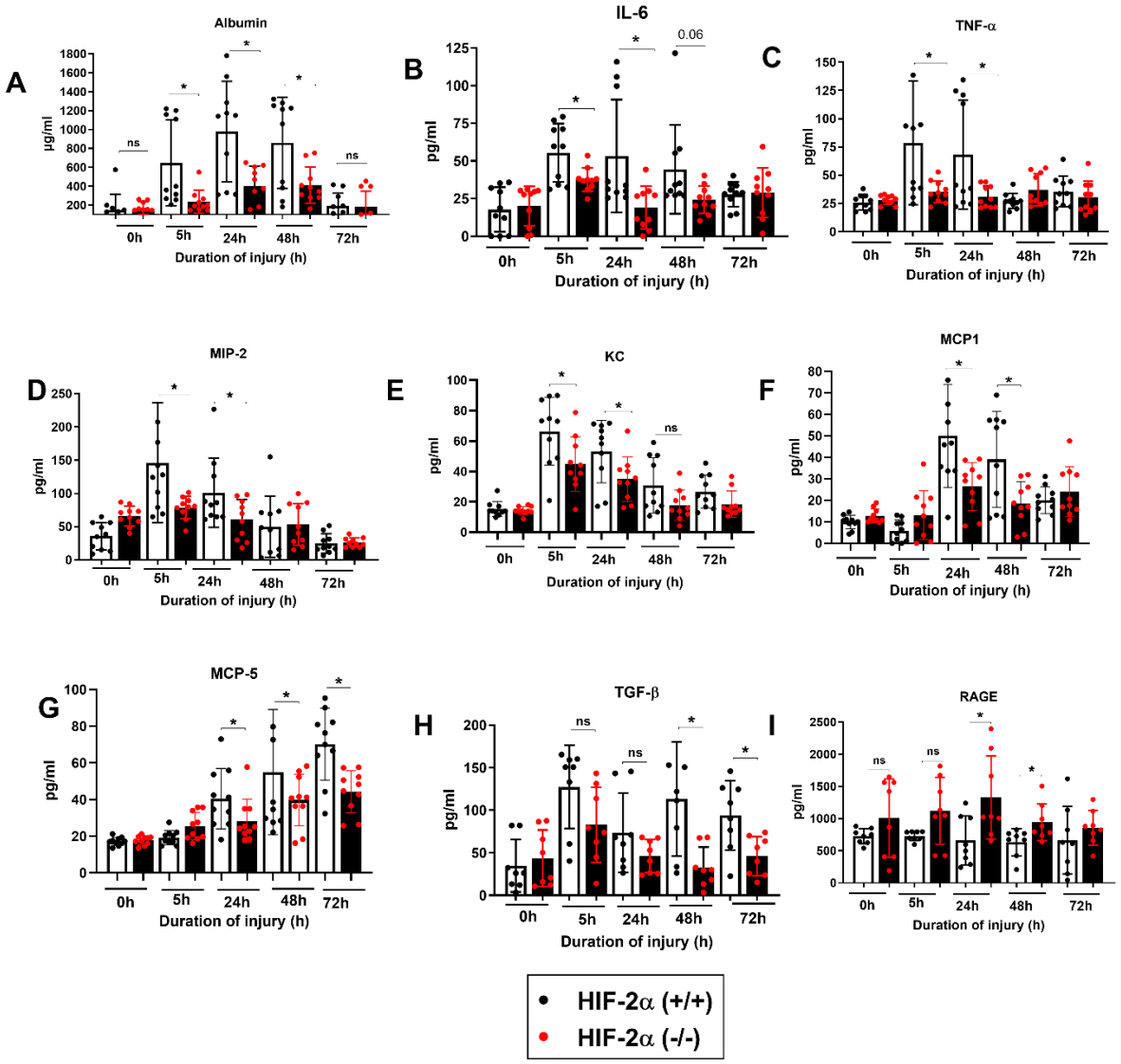

A
Albumin
μg/ml
ns
*
*
*
ns
0h
5h
24h
48h
72h
Duration of injury (h)
B
IL-6
pg/ml
*
*
0.06
0h
5h
24h
48h
72h
Duration of injury (h)
C
TNF-α
pg/ml
*
*
0h
5h
24h
48h
72h
Duration of injury (h)
D
MIP-2
pg/ml
*
*
0h
5h
24h
48h
72h
Duration of injury (h)
E
KC
pg/ml
*
*
ns
0h
5h
24h
48h
72h
Duration of injury (h)
F
MCP1
pg/ml
*
*
0h
5h
24h
48h
72h
Duration of injury (h)
G
MCP-5
pg/ml
*
*
*
0h
5h
24h
48h
72h
Duration of injury (h)
H
TGF-β
pg/ml
ns
ns
*
*
0h
5h
24h
48h
72h
Duration of injury (h)
I
RAGE
pg/ml
ns
ns
*
*
0h
5h
24h
48h
72h
Duration of injury (h)
HIF-2α (+/+)
HIF-2α (-/-)

**Figure 5**

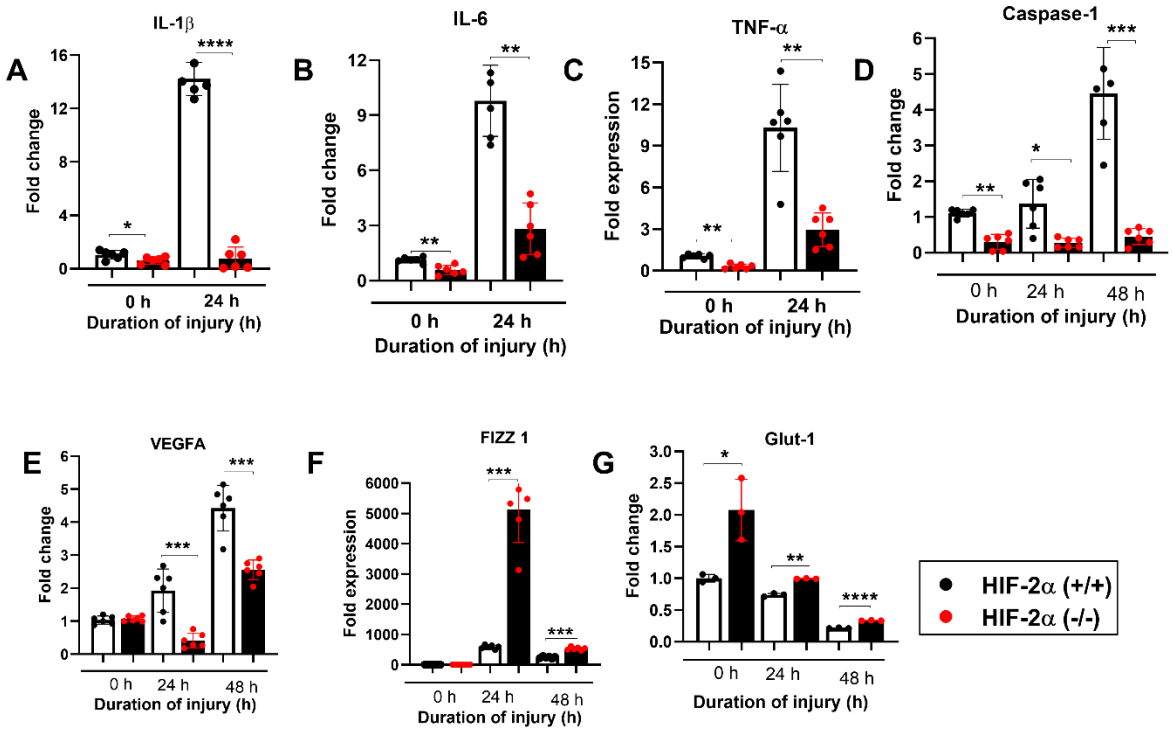

A
IL-1β
Fold change
Duration of injury (h)
0 h
24 h
B
IL-6
Fold change
Duration of injury (h)
C
TNF-α
Fold expression
Duration of injury (h)
D
Caspase-1
Fold change
Duration of injury (h)
48 h
E
VEGFA
Fold change
Duration of injury (h)
F
FIZZ 1
Fold expression
Duration of injury (h)
G
Glut-1
Fold change
Duration of injury (h)
HIF-2α (+/+)
HIF-2α (-/-)

**Figure 6**

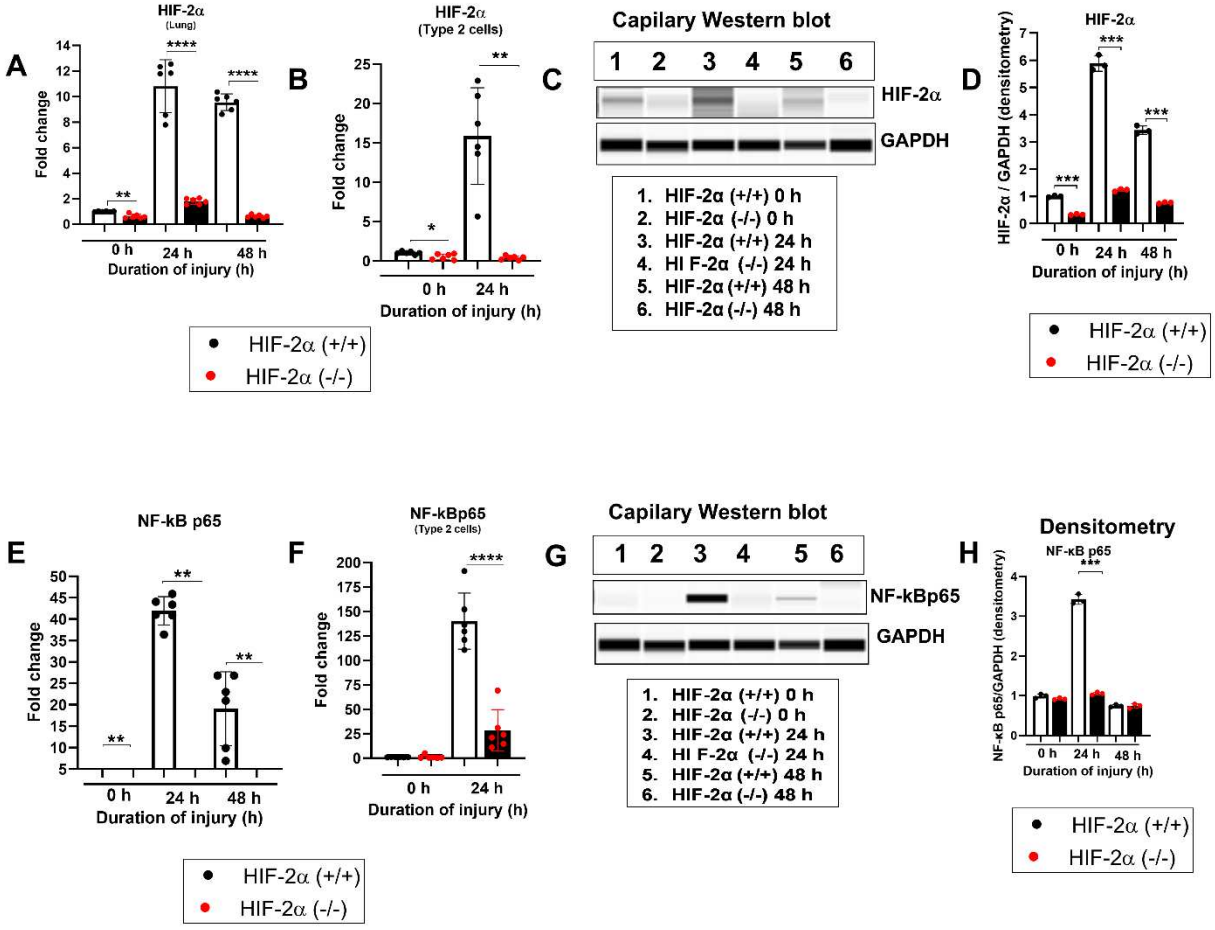

A
HIF-2α
(Lung)
Fold change
Duration of injury (h)
0 h
24 h
48 h
B
HIF-2α
(Type 2 cells)
Fold change
Duration of injury (h)
C
Capilary Western blot
1 2 3 4 5 6
HIF-2α
GAPDH
1. HIF-2α (+/+) 0 h
2. HIF-2α (-/-) 0 h
3. HIF-2α (+/+) 24 h
4. HI F-2α (-/-) 24 h
5. HIF-2α (+/+) 48 h
6. HIF-2α (-/-) 48 h
D
HIF-2α
HIF-2α / GAPDH (densitometry)
Duration of injury (h)
HIF-2α (+/+)
HIF-2α (-/-)
E
NF-kB p65
Fold change
Duration of injury (h)
F
NF-kBp65
(Type 2 cells)
Fold change
Duration of injury (h)
G
Capilary Western blot
1 2 3 4 5 6
NF-kBp65
GAPDH
1. HIF-2α (+/+) 0 h
2. HIF-2α (-/-) 0 h
3. HIF-2α (+/+) 24 h
4. HI F-2α (-/-) 24 h
5. HIF-2α (+/+) 48 h
6. HIF-2α (-/-) 48 h
H
Densitometry
NF-κB p65
NF-κB p65/GAPDH (densitometry)
Duration of injury (h)
HIF-2α (+/+)
HIF-2α (-/-)

**Figure 7**

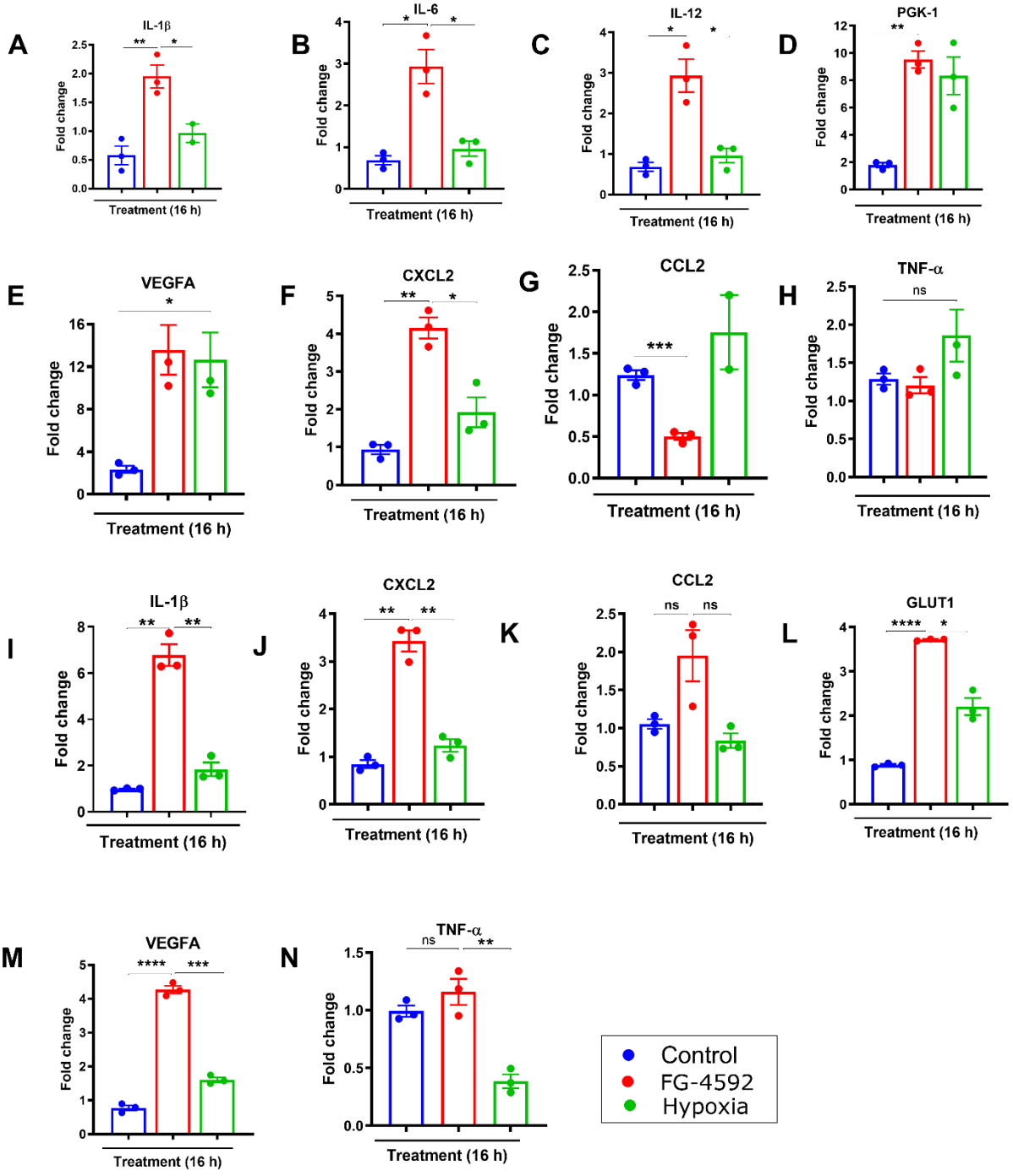

A
IL-1β
B
IL-6
C
IL-12
D
PGK-1
E
VEGFA
F
CXCL2
G
CCL2
H
TNF-α
I
IL-1β
J
CXCL2
K
CCL2
L
GLUT1
M
VEGFA
N
TNF-α
Fold change
Treatment (16 h)
ns
Control
FG-4592
Hypoxia

**Figure 8**

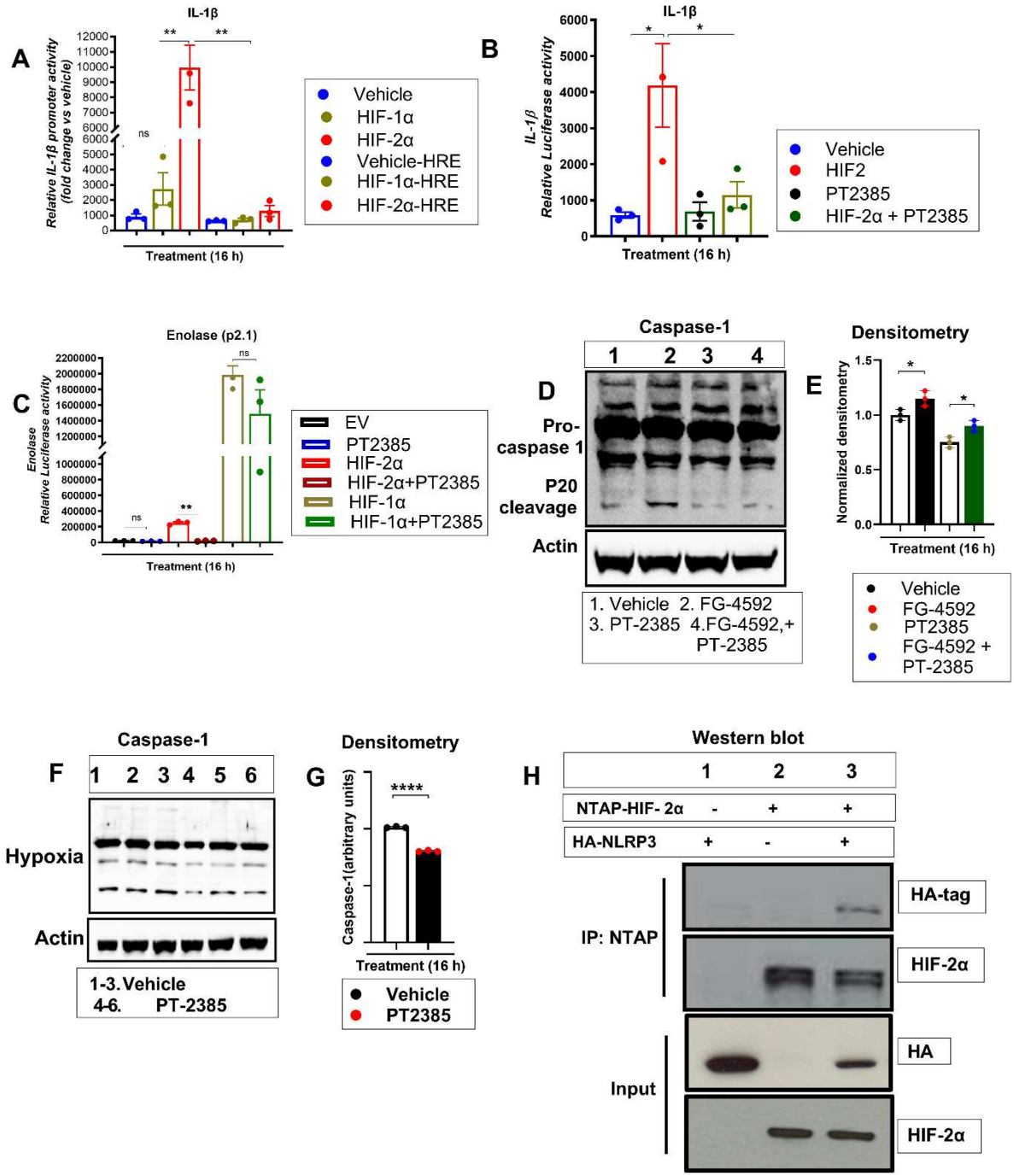

A
IL-1β
Relative IL-1β promoter activity (fold change vs vehicle)
Treatment (16 h)
Vehicle
HIF-1α
HIF-2α
Vehicle-HRE
HIF-1α-HRE
HIF-2α-HRE
B
IL-1β
Relative Luciferase activity
Treatment (16 h)
Vehicle
HIF2
PT2385
HIF-2α + PT2385
C
Enolase (p2.1)
Enolase Relative Luciferase activity
Treatment (16 h)
EV
PT2385
HIF-2α
HIF-2α+PT2385
HIF-1α
HIF-1α+PT2385
D
Caspase-1
1 2 3 4
Pro-caspase 1
P20 cleavage
Actin
1. Vehicle 2. FG-4592
3. PT-2385 4.FG-4592,+ PT-2385
E
Densitometry
Normalized densitometry
Treatment (16 h)
Vehicle
FG-4592
PT2385
FG-4592 + PT-2385
F
Caspase-1
1 2 3 4 5 6
Hypoxia
Actin
1-3.Vehicle
4-6. PT-2385
G
Densitometry
Caspase-1(arbitrary units)
Treatment (16 h)
Vehicle
PT2385
H
Western blot
1 2 3
NTAP-HIF- 2α - + +
HA-NLRP3 + - +
IP: NTAP
HA-tag
HIF-2α
Input
HA
HIF-2α

**Figure 9**

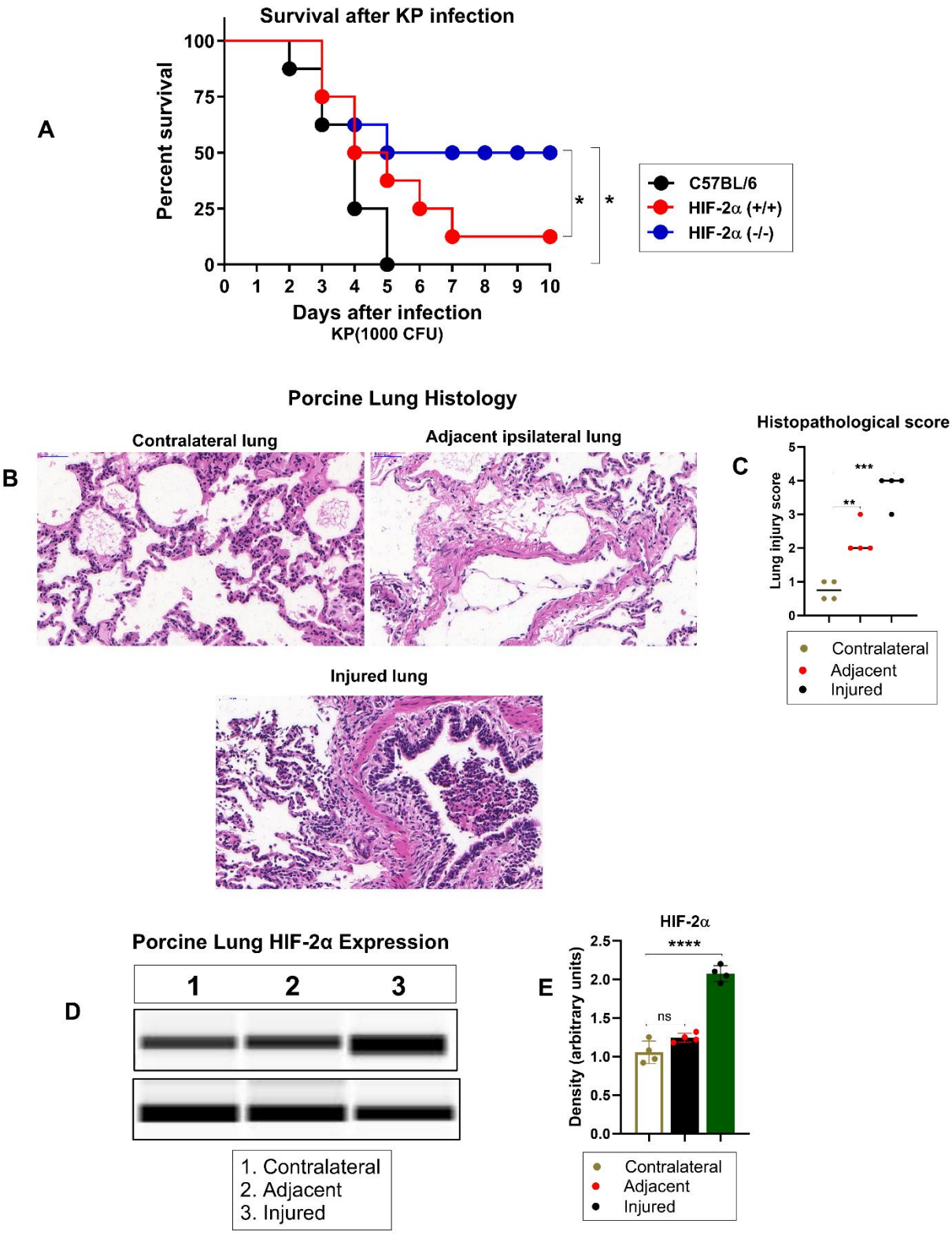
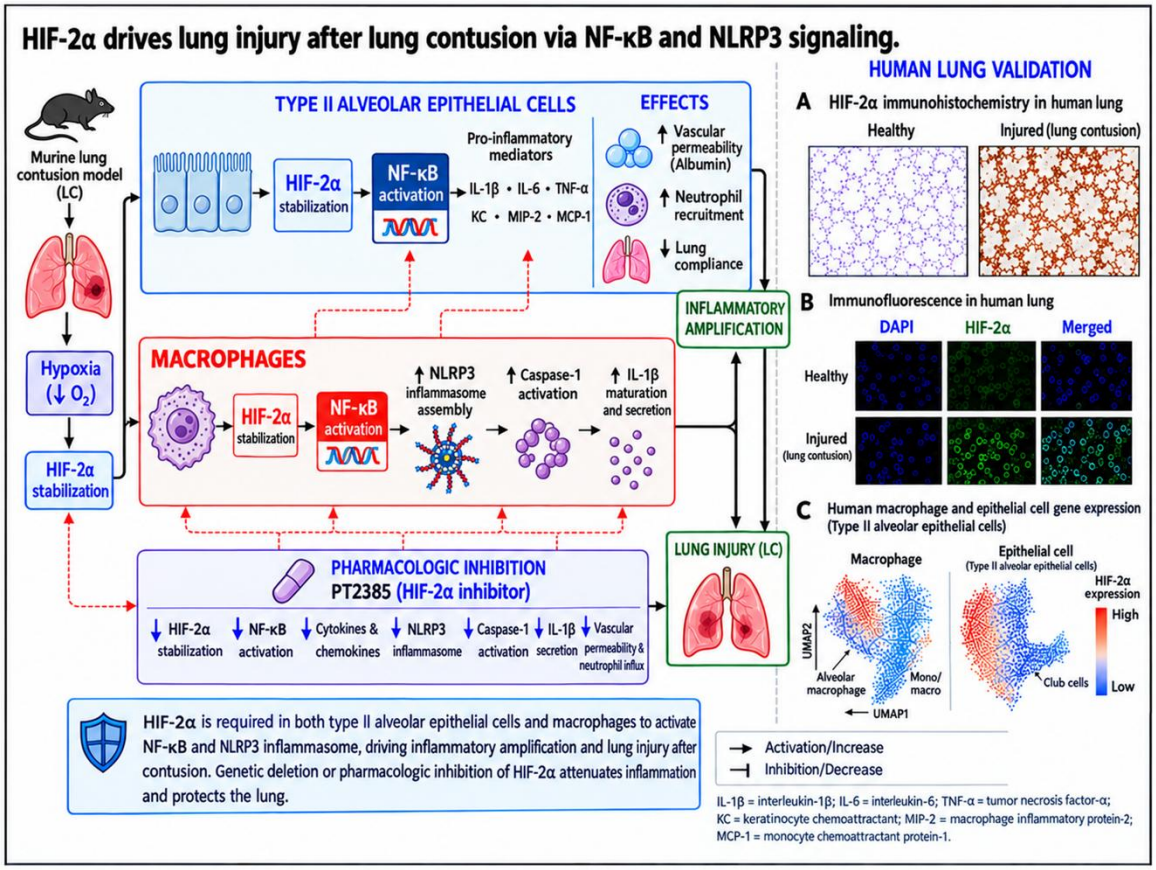

A
Survival after KP infection
Percent survival
100
75
50
25
0
0 1 2 3 4 5 6 7 8 9 10
Days after infection
KP(1000 CFU)
*
*
C57BL/6
HIF-2α (+/+)
HIF-2α (-/-)
B
Porcine Lung Histology
Contralateral lung
Adjacent ipsilateral lung
Injured lung
C
Histopathological score
Lung injury score
***
**
Contralateral
Adjacent
Injured
D
Porcine Lung HIF-2α Expression
1
2
3
1. Contralateral
2. Adjacent
3. Injured
E
HIF-2α
****
ns
Density (arbitrary units)
2.5
2.0
1.5
1.0
0.5
0.0
Contralateral
Adjacent
Injured

**Figure 10**


HIF-2α drives lung injury after lung contusion via NF-κB and NLRP3 signaling.
Murine lung contusion model (LC)
Hypoxia (↓ O2)
HIF-2α stabilization
TYPE II ALVEOLAR EPITHELIAL CELLS
HIF-2α stabilization
NF-κB activation
Pro-inflammatory mediators
IL-1β • IL-6 • TNF-α
KC • MIP-2 • MCP-1
EFFECTS
↑ Vascular permeability (Albumin)
↑ Neutrophil recruitment
↓ Lung compliance
INFLAMMATORY AMPLIFICATION
MACROPHAGES
HIF-2α stabilization
NF-κB activation
↑ NLRP3 inflammasome assembly
↑ Caspase-1 activation
↑ IL-1β maturation and secretion
PHARMACOLOGIC INHIBITION
PT2385 (HIF-2α inhibitor)
↓ HIF-2α stabilization
↓ NF-κB activation
↓ Cytokines & chemokines
↓ NLRP3 inflammasome
↓ Caspase-1 activation
↓ IL-1β secretion
↓ Vascular permeability & neutrophil influx
LUNG INJURY (LC)
HIF-2α is required in both type II alveolar epithelial cells and macrophages to activate NF-κB and NLRP3 inflammasome, driving inflammatory amplification and lung injury after contusion. Genetic deletion or pharmacologic inhibition of HIF-2α attenuates inflammation and protects the lung.
HUMAN LUNG VALIDATION
A HIF-2α immunohistochemistry in human lung
Healthy
Injured (lung contusion)
B Immunofluorescence in human lung
DAPI
HIF-2α
Merged
Healthy
Injured (lung contusion)
C Human macrophage and epithelial cell gene expression (Type II alveolar epithelial cells)
Macrophage
Epithelial cell (Type II alveolar epithelial cells)
HIF-2α expression
High
Low
UMAP2
UMAP1
Alveolar macrophage
Mono/ macro
Club cells
Activation/Increase
Inhibition/Decrease
IL-1β = interleukin-1β; IL-6 = interleukin-6; TNF-α = tumor necrosis factor-α; KC = keratinocyte chemoattractant; MIP-2 = macrophage inflammatory protein-2; MCP-1 = monocyte chemoattractant protein-1.